

Piperazine-2,3-dicarboxylic Acid Derivatives as Dual Antagonists of NMDA and GluK1-Containing Kainate Receptors

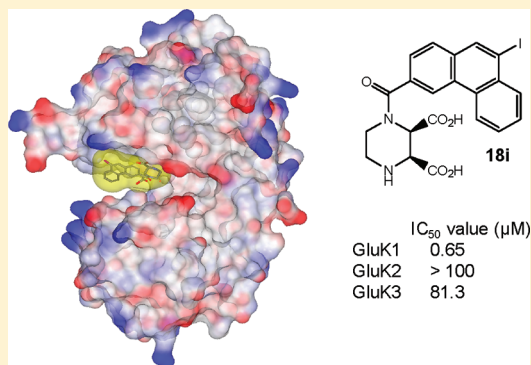
Mark W. Irvine,^{†,||} Blaise M. Costa,^{§,||} Daniel Dlaboga,[†] Georgia R. Culley,[†] Richard Hulse,[‡] Caroline L. Scholefield,[†] Palmi Atlason,[†] Guangyu Fang,[†] Richard Eaves,[†] Richard Morley,[†] Maria B. Mayo-Martin,[†] Mascia Amici,[†] Zuner A. Bortolotto,[†] Lucy Donaldson,[‡] Graham L. Collingridge,[†] Elek Molnár,[†] Daniel T. Monaghan,^{§,||} and David E. Jane^{*,†,||}

[†]MRC Centre for Synaptic Plasticity and [‡]School of Physiology and Pharmacology, University of Bristol, Medical Sciences Building, University Walk, Bristol, BS8 1TD, U.K.

[§]Department of Pharmacology and Experimental Neuroscience, University of Nebraska Medical Center, Omaha, Nebraska 68198-6260, United States

Supporting Information

ABSTRACT: Competitive *N*-methyl-D-aspartate receptor (NMDAR) antagonists bind to the GluN2 subunit, of which there are four types (GluN2A–D). We report that some *N*¹-substituted derivatives of *cis*-piperazine-2,3-dicarboxylic acid display improved relative affinity for GluN2C and GluN2D versus GluN2A and GluN2B. These derivatives also display subtype selectivity among the more distantly related kainate receptor family. Compounds **18i** and (–)-**4** were the most potent kainate receptor antagonists, and **18i** was selective for GluK1 versus GluK2, GluK3 and AMPA receptors. Modeling studies revealed structural features required for activity at GluK1 subunits and suggested that S674 was vital for antagonist activity. Consistent with this hypothesis, replacing the equivalent residue in GluK3 (alanine) with a serine imparts **18i** antagonist activity. Antagonists with dual GluN2D and GluK1 antagonist activity may have beneficial effects in various neurological disorders. Consistent with this idea, antagonist **18i** (30 mg/kg ip) showed antinociceptive effects in an animal model of mild nerve injury.



INTRODUCTION

Inotropic glutamate receptors (iGluRs) are L-glutamate-gated ion channels that mediate fast synaptic transmission in the central nervous system (CNS). There are three groups of iGluRs named after compounds by which they are selectively activated: AMPA ((*S*)-2-amino-3-hydroxy-5-methyl-4-isoxazolepropanoic acid), kainate ((2*S*,3*S*,4*S*)-3-carboxymethyl-4-isopropenylpyrrolidine-2-carboxylic acid), and NMDA (*N*-methyl-D-aspartic acid) receptors.¹ Kainate receptors (KARs) are tetrameric assemblies of GluK1–5 subunits (IUPHAR nomenclature of the receptors that were previously known as GluR5–7, KA1, and KA2).² AMPA receptors (AMPA receptors) are tetrameric assemblies of a combination of GluA1–4 subunits (IUPHAR nomenclature of the receptors that were previously known as GluR1–4 or GluRA–D),² while NMDAR tetramers can be assembled from GluN1, GluN2A–D and in some areas of the CNS, GluN3A and GluN3B subunits (IUPHAR nomenclature of the receptors that were previously known as NR1, NR2A–D and NR3A and NR3B).^{1–3}

NMDARs have been the subject of intense investigations into the development of antagonists because of the implication of these receptors in neurological disorders such as epilepsy and chronic pain and neurodegenerative disorders such as ischemia

and Alzheimer's and Parkinson's diseases.⁴ Antagonists interacting with the glutamate binding site on GluN2 subunits, the glycine binding site on GluN1 subunits, the ion channel pore, and the N-terminal domain of the GluN2B subunit have been developed.^{1–3} Most antagonists interacting at the orthosteric glutamate binding site on GluN2 subunits such as **1**, **2**, and **3** (Figure 1) display the following rank order of affinity: GluN2A > GluN2B > GluN2C > GluN2D.³ We have reported that piperazine-2,3-dicarboxylic acid derivatives such as (±)-**4** and **5** (Figure 1) show a different rank order of affinity: GluN2D ~ GluN2C > GluN2B > GluN2A.^{5,6} Negative allosteric modulators have been reported that have greater GluN2 subunit selectivity than that reported for competitive antagonists. For example, **6** binds selectively to the N-terminal domain of GluN2B,⁷ and **7**⁸ and **8**⁹ (Figure 1) selectively block GluN2C/GluN2D versus GluN2A and GluN2B.

The first antagonists with significant activity at KARs were from the quinoxalinedione class of compounds, such as the potent AMPAR antagonist 2,3-dihydroxy-6-nitro-7-sulfamoylbenzo(*f*)-quinoxaline (**9**) (Figure 1).¹⁰ Quinoxalinediones were not useful

Received: September 15, 2011

Published: November 24, 2011

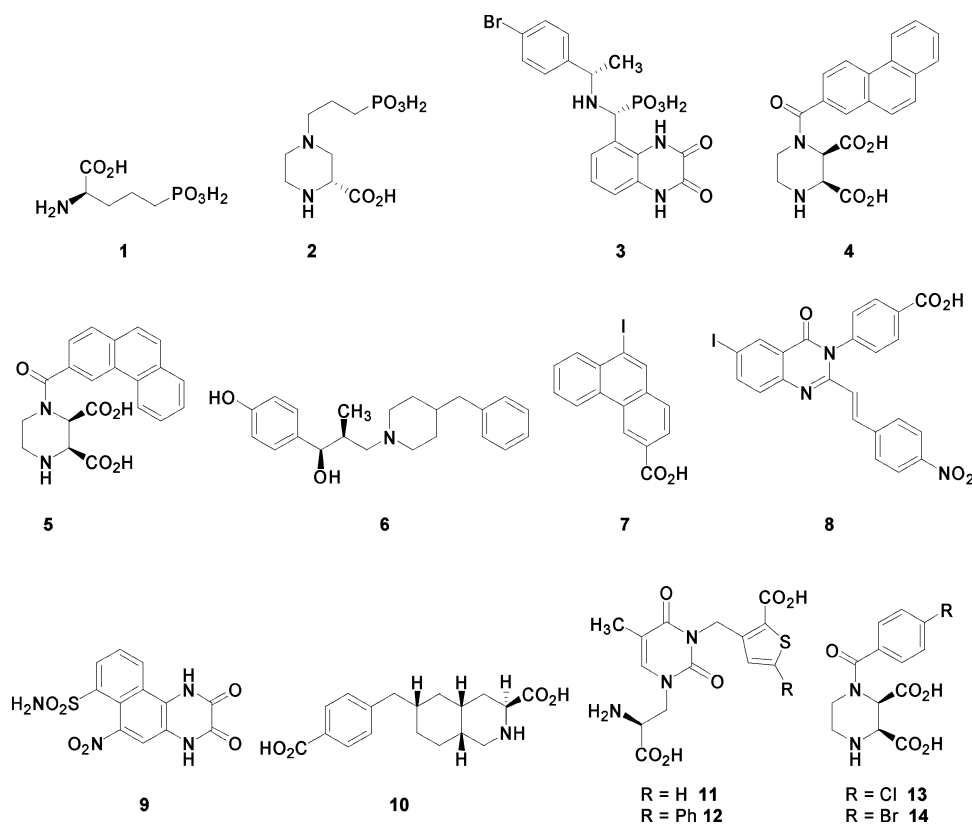


Figure 1. Structures of known NMDAR and KAR antagonists.

as pharmacological tools for KARs, as they also antagonized AMPARs. More recently a series of decahydroisoquinolines, such as **10** (Figure 1), have been reported as selective GluK1-containing KAR antagonists.^{11,12} These antagonists displayed selectivity for GluK1 versus GluK2-containing KARs and AMPARs and were therefore used to provide evidence to support the role of GluK1 in synaptic plasticity in the mossy fiber to CA3 region of the hippocampus and in a number of CNS disorders such as chronic pain, epilepsy, ischemia, and migraine.^{2b,11,12} The activity of decahydroisoquinolines on GluK3 is not well established, as only **10** (Figure 1) has been tested on GluK3 to date. Compound **10** was found to have no activity on homomeric GluK3 at the concentration at which it is used to block GluK1 in physiological experiments.¹³

We have reported that derivatives of the natural product willardiine, such as **11** and **12** (Figure 1), are selective GluK1-containing KAR antagonists.¹⁴ Compounds from this series have been used to implicate GluK1-containing KARs in the induction of long-term potentiation (LTP) in the mossy fiber to CA3 pathway in the hippocampus and in short-term recognition memory.¹⁵ Derivatives of the natural product willardiine, such as **11** and **12**, are selective for GluK1-containing receptors over GluK2,¹⁴ but these compounds also potently antagonize homomeric GluK3 receptors.¹³

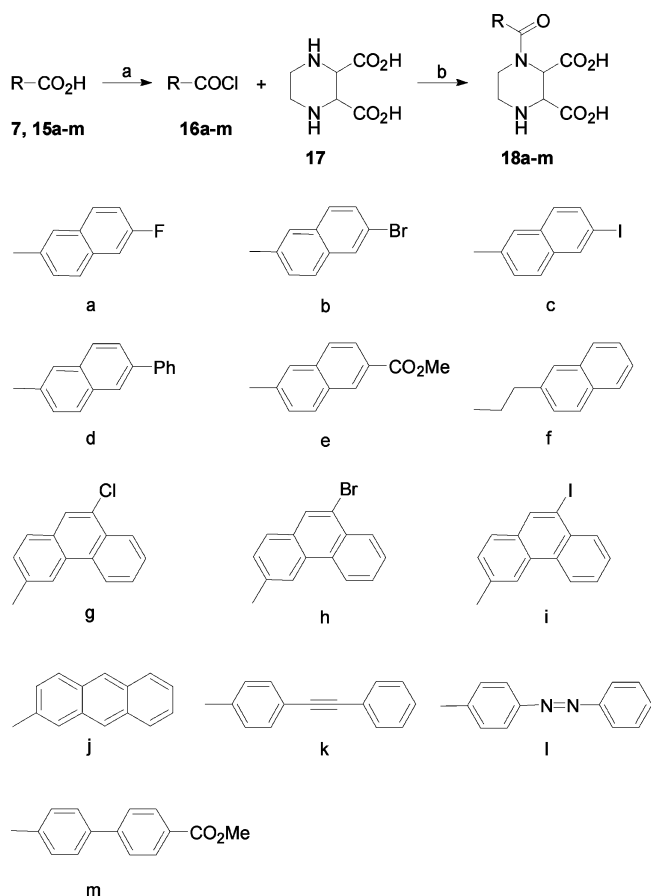
Two *N*¹-substituted piperazine-2,3-dicarboxylates **13** and **14** (Figure 1) have been shown to be broad spectrum iGluR antagonists that bind to both NMDARs and KARs.¹⁶ Herein we report the synthesis and pharmacological characterization of a new series of analogues of **13** and **14**, which show moderate selectivity for GluN2C/GluN2D versus GluN2A/GluN2B and in the case of one of the more potent GluK1 antagonists identified in this study, excellent selectivity for GluK1 versus

GluK2 and GluK3. Molecular modeling studies using the X-ray crystal structure of the antagonist bound form of the ligand binding domain (LBD) of GluK1 have been used to investigate the binding modes of some compounds in GluK1. The proposed GluK1 binding model was then tested by site-directed mutagenesis. Given that both GluK1 and GluN2D have been implicated in neuropathic pain,^{4b,11e,f,12b} we tested a compound that is a dual antagonist of GluN2D and GluK1 in an animal model of mild nerve injury to assess antinociceptive activity.

RESULTS

Chemistry. A series of *N*¹-substituted piperazine-2,3-dicarboxylic acid derivatives (**18a–m**) were synthesized by reacting various acid chlorides (**16a–m**) with the *cis*-isomer of **17** under modified Schotten–Baumann conditions (Scheme 1).⁶ The acid chlorides (**16a–m**) were prepared from the corresponding carboxylic acids (**7**, **15a–m**) by treatment with excess thionyl chloride. The only exception to this was **16l**, which was purchased commercially. Carboxylic acids **15a**, **15b**, **15e**,¹⁷ **15f**,¹⁸ **15j**, and **15m** where either available commercially or synthesized via published procedures. The naphthyl and biphenyl carboxylic acid compounds (**19** and **20**) were synthesized via base hydrolysis of the corresponding esters (**18e** and **18m**). Hydrogenation of the alkyne linker in **18k** afforded phenethyl derivative **21** (Scheme 2).

6-Iodo-2-naphthoic acid (**15c**) has previously been synthesized from *N*-acetyl-2-naphthylamine via a time-consuming seven-step route.¹⁹ However, by utilizing an aromatic Finkelstein reaction to convert methyl 6-bromo-2-naphthoate (**22**) to its corresponding iodo analogue (**23**) and then hydrolyzing the ester, we were able to generate **15c** in only two steps (Scheme 3). Suzuki coupling between **22** and phenylboronic acid afforded

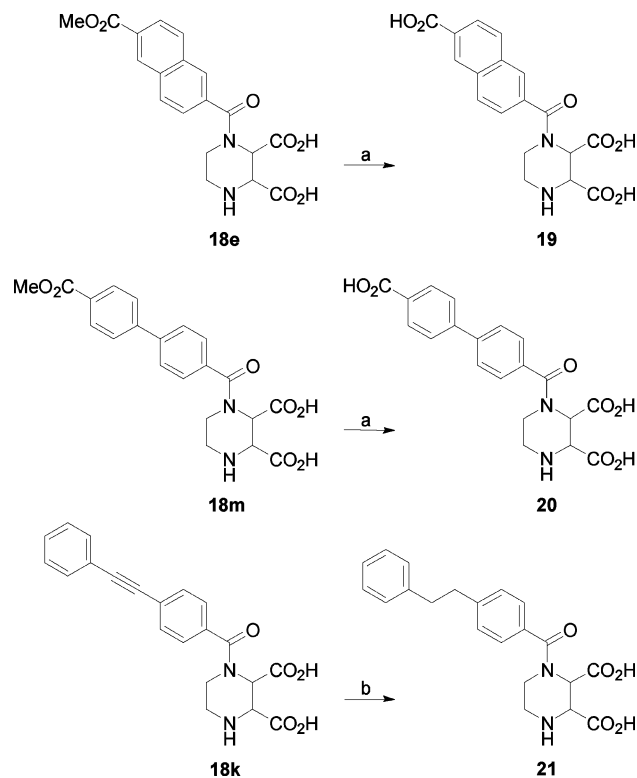
Scheme 1^a

^aReagents and conditions: (a) (i) SOCl_2 , C_6H_6 or dioxane, reflux, 12 h; (b) (i) 3 equiv of NaOH , dioxane/ H_2O (2:1), 0°C , 2 h, and then rt, 4 h; (ii) 2 M HCl (aq).

ester **24** which was subsequently hydrolyzed to **15d** (Scheme 3). Sonogashira coupling followed by a haloform reaction was employed to convert 4-iodoacetophenone (**25**) to acetylene acid **15k** (Scheme 4).

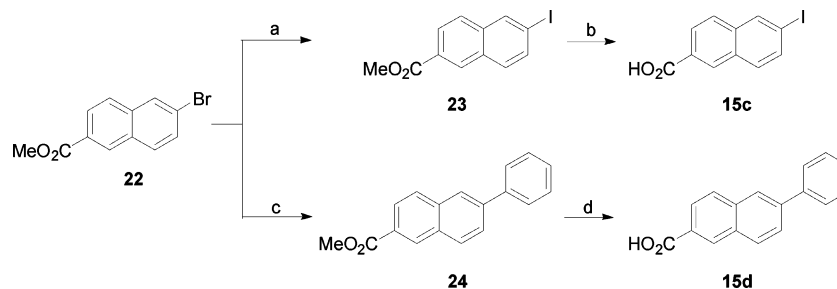
The 3-acetyl derivatives of 9-chloro and 9-bromophenanthrene (**27** and **28**) were synthesized by Friedel–Crafts acylation as described previously.^{20,21} Unfortunately, attempts to utilize the same conditions to synthesize the 3-acetyl derivative of 9-iodophenanthrene failed and led only to the isolation of a black tar. Attempts to modify the reaction conditions by using aluminum iodide instead of aluminum chloride or acetic anhydride instead of acetyl chloride led only to the same outcome. Consequently, we employed an aromatic Finkelstein reaction²² to convert 3-acetyl-9-bromophenanthrene (**28**) to its corresponding 9-iodo analogue (**29**). The acetyl compounds (**27–29**) were conveniently converted to the desired phenanthrene acids (**7**, **15g**, **15h**) by reaction with sodium hypobromite in a modified haloform reaction (Scheme 5).

Resolution of (\pm)-**4** was achieved by forming diastereomeric salts with the individual enantiomers of 1-phenethylamine (**32** and **33**) (Scheme 6). In each case, the isolated diastereomeric salts were crystallized to constant rotation to provide the pure diastereoisomers (**30** and **31**). These were then individually dissolved in $\text{THF}/\text{H}_2\text{O}$ and acidified with aqueous hydrochloric acid to afford the free acids of each enantiomer (($-$)-**4** and ($+$)-**4**, Scheme 6) in good yield.

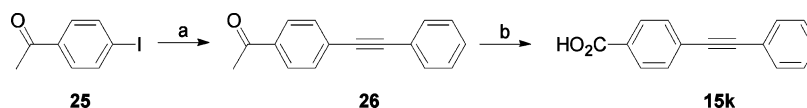
Scheme 2^a

^aReagents and conditions: (a) (i) LiOH , H_2O , room temp, 4 h; (ii) 2 M HCl (aq); (b) (i) 10% Pd/C , H_2 , NaOH , H_2O , room temp, 18 h; (ii) 2 M HCl (aq).

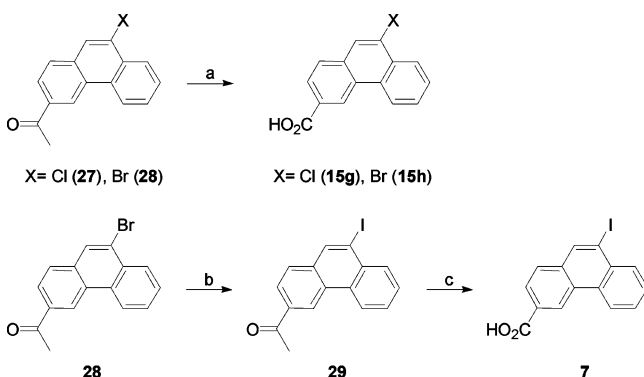
Electrophysiological Assays on Recombinant Rat NMDAR Subtypes Expressed in *Xenopus* Oocytes. We have reported previously that piperazine-2,3-dicarboxylic acids substituted at the N^1 position with bulky aromatic substituents show an unusual pattern of GluN2 subunit selectivity.^{5,6} The vast majority of competitive antagonists, such as compounds **1** and **2** (Figure 1), display the following rank order of affinity: $\text{GluN2A} > \text{GluN2B} > \text{GluN2C} > \text{GluN2D}$.³ However, compounds (\pm)-**4** and **5** (Figure 1) display the opposite rank order of affinity: $\text{GluN2D} \sim \text{GluN2C} > \text{GluN2B} > \text{GluN2A}$, though the degree of separation between GluN2 subunits is only up to ~ 10 -fold. We have proposed that this altered selectivity is due to the large phenanthrene group extending out of the highly conserved glutamate binding pocket and interacting with subunit-specific elements in the receptor.^{5,6,23} We have synthesized several novel compounds with modifications to the phenanthrene ring to gain more insight into the structural requirements for GluN2 subunit selectivity, with the focus being on developing GluN2D subunit selective competitive antagonists. We also sought to define their actions at the more distantly related KAR family. The new compounds (($-$)-**4**, ($+$)-**4**, **18a–d**, **18f**, **18g–I**, **19–21**, Tables 1 and 2) were tested on GluN1a in combination with each of the four genetically distinct subunits, GluN2A–D, expressed in *Xenopus* oocytes in an electrophysiological assay using two-electrode voltage clamp. The IC_{50} values that were determined for the ability of the compounds to block a response evoked by $10\ \mu\text{M}$ L-glutamate and $10\ \mu\text{M}$ glycine were converted to K_i values to take into account the differences in agonist potency for the individual GluN2 subtypes.

Scheme 3^a

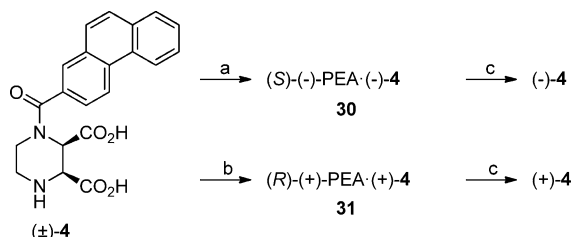
^aReagents and conditions: (a) NaI, CuI, *N,N'*-dimethylethylenediamine, dioxane, 110 °C, 65 h; (b) (i) KOH, dioxane, 70 °C, 2 h; (ii) 2 M HCl (aq); (c) Ph-B(OH)₂, K₂CO₃, Pd(PPh₃)₄, toluene/ethanol/water (4:1:2), 80 °C, 18 h; (d) (i) NaOH, THF/H₂O, 70 °C, 2 h; (ii) 2 M HCl (aq).

Scheme 4^a

^aReagents and conditions: (a) phenylacetylene, CuI, PdCl₂(PPh₃)₂, TBAF, THF, room temp, 18 h; (b) (i) Br₂, NaOH, dioxane, 70 °C, 1 h; (ii) conc H₂SO₄.

Scheme 5^a

^aReagents and conditions: (a) (i) Br₂, NaOH, dioxane, 70 °C, 1 h; (ii) conc HCl (aq); (b) NaI, CuI, *N,N'*-dimethylethylenediamine, dioxane, 110 °C, 65 h; (c) (i) Br₂, NaOH, dioxane, 70 °C, 1 h; (ii) conc HCl (aq).

Scheme 6^a

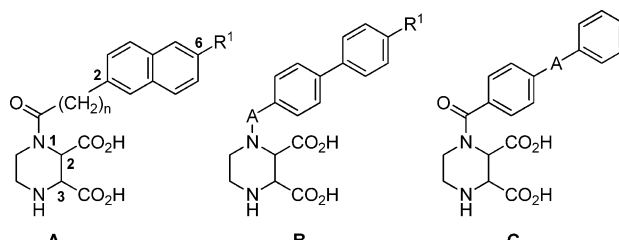
^aReagents and conditions: (a) (i) (*S*)-(-)-1-phenethylamine (32), dioxane/H₂O (1:1), room temp, 30 min; (ii) crystallization (dioxane/water); (b) (i) (*R*)-(+)-1-phenylethylamine (33), dioxane/H₂O (1:1), room temp, 18 h; (ii) crystallization (dioxane/water); (c) THF/H₂O, 2 M HCl (aq).

When the individual enantiomers of (±)-4 were tested, it was found that the high affinity GluN2D binding resided in the (-)-4 isomer with the (+)-4 isomer displaying 50-fold lower affinity for GluN2D (Table 2). However, (-)-4 showed no

improvement in GluN2D selectivity compared to (±)-4. We have demonstrated previously that a three-ring aromatic substituent is required for optimal affinity and selectivity for GluN2D.^{5,6} A phenanthrene ring attached at the 3-position to the carbonyl group, as in 5 (Table 2), is most favored for GluN2D subunit selectivity, albeit with reduced GluN2D affinity compared to (±)-4.^{5,6} For a series of 9-halo-substituted phenanthrene derivatives (18g–i, Table 2) of 5 the rank order of affinity for each of the four GluN2s was I > Br > Cl > H. The most GluN2D selective compounds were the parent compound 5 and the 9-bromo derivative 18h. These compounds showed 10- and 7-fold selectivity for GluN2D versus GluN2A and GluN2B, respectively, but showed only 2-fold selectivity for GluN2D versus GluN2C. Thus, substitution at the 9-position has little impact on GluN2D affinity but GluN2D selectivity varies with the nature of the substituent. Replacement of the phenanthrene ring of (±)-4 with an anthracene ring to give 18j did not improve affinity or selectivity for GluN2D (Table 2).

To determine whether a linker could replace the middle ring of (±)-4, we tested analogues in which the first and last benzene rings were separated with an acetylene (18k), ethylene (21), or diazene (18l) linker (Table 1). These substitutions were found to be detrimental; each of these compounds had low affinity for GluN2D, with 21 having much reduced GluN2D potency compared to (±)-4 (21 (100 μM) showed only ~10% antagonism of agonist induced effects on GluN2D). 18l and 18k showed partial GluN2D selectivity, with ~10-fold selectivity for GluN2D versus GluN2A, but they did not differentiate between GluN2D and GluN2B or GluN2C. Replacement of the first phenyl ring of (±)-4 with an ethylene spacer to give 18f reduced GluN2D affinity and selectivity (Table 1).

A series of 6-substituted naphthalene derivatives (18a–d, 19, Table 1) were tested to determine if the 6-substituent could replace the third benzene ring of (±)-4. The rank order of affinity of the 6-substituted naphthalene derivatives for GluN2D was I > Br > Ph > F > H > CO₂H. The higher affinity observed for naphthalene derivatives bearing lipophilic substituents compared to polar substituents suggests that the

Table 1. Summary of the Activity of Piperazine-2,3-dicarboxylic Acid Derivatives at Recombinant NMDAR and KAR Subtypes^a


compd	formula	n	A	R ¹	NMDAR K _i , μM (n ≥ 4) ^b				KAR K _B , μM (n = 3) ^c	
					GluN2A	GluN2B	GluN2C	GluN2D	GluK1	GluK2
34a ^d	A	0		H	9.6 ± 1.1	18.2 ± 1.3	3.9 ± 0.1	9.3 ± 0.4	45.6 ± 11.5	ND
18a	A	0		F	7.4 ± 1.5	12.3 ± 0.9	3.6 ± 0.1	5.1 ± 0.1	52.9 ± 3.9	ND
18b	A	0		Br	4.1 ± 0.3	2.7 ± 0.2	2.1 ± 0.1	2.2 ± 0.1	16.2 ± 3.6	ND
18c	A	0		I	3.0 ± 0.2	1.3 ± 0.1	1.8 ± 0.1	1.6 ± 0.1	7.5 ± 1.4	>100
18d	A	0		Ph	>100 ^e	>100 ^e	5.1 ± 0.1	2.4 ± 0.1	5.8 ± 1.5	>100
18f	A	2		H	5.1 ± 0.5	2.3 ± 0.2	4.1 ± 0.3	2.7 ± 0.2	67.8 ± 5.2	ND
19	A	0		CO ₂ H	>100 ^f	>100 ^f	>100 ^f	>100 ^f	59.7 ± 2.0	ND
34b ^d	B		CO	H	15.7 ± 0.4	5.0 ± 0.3	9.0 ± 0.2	4.3 ± 0.1	9.8 ± 1.4	>100
34c ^d	B		SO ₂	H	13.6 ± 1.8	16.2 ± 4.1	8.7 ± 0.6	10.9 ± 0.5	>100	ND
20	B		CO	CO ₂ H	ND	>100 ^g	>100 ^g	ND	51.5 ± 18.7	ND
18k	C		C≡C		138 ± 9	24.1 ± 1.1	21.4 ± 0.4	10.5 ± 1.3	13.4 ± 3.3	>100
18l	C		N=N		99.3 ± 7.0	12.9 ± 1.4	28.0 ± 1.0	10.8 ± 0.3	14.2 ± 3.1	>100
21	C		(CH ₂) ₂		>100 ^h	>100 ^h	>100 ^h	>100 ^h	16.7 ± 3.4	ND

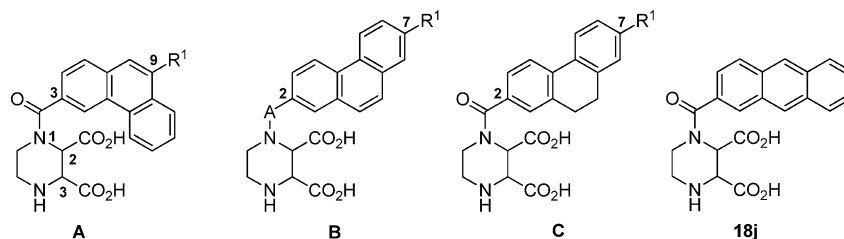
^aAbbreviations: ND = not determined. ^bK_i values (μM) for inhibiting the responses of recombinant rat NMDA receptors (GluN1 expressed with the appropriate GluN2 subunit) expressed in *Xenopus* oocytes (mean ± SEM). For compounds with activities listed as >100 this refers to the IC₅₀ value. ^cK_B values for antagonism of glutamate-stimulated Ca²⁺ influx in HEK293 cells expressing either human GluK1 or GluK2 (mean ± SEM). For compounds with activities listed as >100 this refers to the K_B value. ^dData for NMDA activity taken from ref 6. ^e30.3 ± 8.2% and 37.1 ± 5.0% antagonism of GluN2A and GluN2B, respectively at 100 μM 18d. ^fLess than 5% antagonism of GluN2A-D at 100 μM 19. ^gLess than 15% antagonism of GluN2B and GluN2C at 100 μM 20. ^h11.50 ± 2.25%, >5%, 29.12 ± 1.00%, and 10.25 ± 1.03% antagonism of GluN2A, GluN2B, GluN2C, and GluN2D, respectively, at 100 μM 21.

6-substituent is in a spacious hydrophobic environment in the GluN2D ligand binding site. A similar marked lowering in GluN2D affinity was observed when a 4'-carboxy substituent was added to the biphenyl derivative 34b leading to compound 20 (Table 1). A number of these compounds had affinity for GluN2D similar to that observed for phenanthrene substituted compounds such as 5 and its derivatives (Table 2), suggesting that the third phenyl ring does not have a major impact on GluN2D affinity. However, the presence of the third phenyl ring improved GluN2D selectivity (e.g., 5 (Table 2) shows much greater GluN2D selectivity than 18b (Table 1)), mainly by reducing affinity for GluN2A and GluN2B. Among the 6-naphthyl derivatives only 18d (Table 1) showed GluN2D selectivity, with only 30–37% antagonism of GluN2A and GluN2B observed when tested at 100 μM. However, this compound did not discriminate between GluN2C and GluN2D. It was not possible to obtain K_i values for antagonism of GluN2A and GluN2B by 18d and to obtain a good estimate of selectivity because of poor solubility at higher concentrations. At 300 μM in the electrophysiological recording buffer at room temperature, the compound displayed visible light scattering and thus the compound was considered insoluble at high concentrations.

Calcium Fluorescence Assays on Human KAR Subtypes. Two benzoylpiperazine-2,3-dicarboxylic acid derivatives 13 and 14 (Figure 1) have been reported to be more potent as antagonists of KARs than NMDARs. However, the interpretation of these experiments is complicated by the use of nonselective agonists in the assays.^{2b,16} To investigate the potential KAR antagonist activity of a range of N¹-substituted

piperazine-2,3-dicarboxylic acids, including the newly synthesized compounds ((-)-4, (+)-4, 18a–d, 18f, 18g–l, 19–21) and those reported previously ((±)-4, 5, 34a–h) (Tables 1 and 2), they were tested on human recombinant GluK1 receptors expressed in human embryonic kidney 293 (HEK293) cells. The IC₅₀ values that were determined for the ability of the compounds to block an increase in Ca²⁺-stimulated fluorescence evoked by 100 μM L-glutamate were converted to K_B values (Tables 1 and 2). Many of the compounds had similar antagonist potency on GluK1 and GluN2D, while other compounds displayed selectivity for GluK1 versus GluN2D or >30-fold selectivity for GluN2D versus GluK1.

Compounds with a 3-ringed aryl substituent were found to be the most potent GluN2D antagonists; however, this feature was less important for activity on GluK1. Thus, (±)-4 (Table 2) had similar affinity for GluK1 to the biphenyl derivative 34b and only 6-fold higher affinity than the naphthyl derivative 34a (Table 1). The interaction of (±)-4 with GluK1 was stereoselective with (±)-4 displaying 8-fold higher affinity than the trans-isomer (34d) and the (-)-4 enantiomer having 27-fold higher affinity than the (+)-4 enantiomer (Table 2). However, the stereoselectivity for binding to GluK1 was not as great as that observed for the interaction of these isomers of (±)-4 with GluN2D. (-)-4 was the most potent GluK1 antagonist tested. However, it had higher affinity for GluN2D and displayed ~30-fold selectivity for GluN2D versus GluK1. 7-Bromo substitution of the phenanthrene ring of (±)-4 to give 34e did not change GluK1 affinity (Table 2). An analogue of (±)-4 with a saturated middle ring (34g) and its 9-bromo

Table 2. Activity of Piperazine-2,3-dicarboxylic Acid Derivatives at Recombinant NMDAR and KAR Subtypes^a

compd	formula	A	R ¹	NMDAR K_{B} μM ($n \geq 4$) ^b				KAR K_{B} μM ($n = 3$) ^c	
				GluN2A	GluN2B	GluN2C	GluN2D	GluK1	GluK2
5 ^d	A		H	22.0 ± 1.4	17.2 ± 1.2	5.2 ± 0.5	2.4 ± 0.1	14.2 ± 3.4	>100
18g	A		Cl	7.2 ± 0.7	15.2 ± 2.6	3.2 ± 0.2	1.7 ± 0.1	21.8 ± 6.0	ND
18h	A		Br	11.5 ± 0.8	8.0 ± 0.4	2.8 ± 0.1	1.2 ± 0.1	12.8 ± 2.1	>100
18i	A		I	7.4 ± 0.9	3.8 ± 0.9	1.9 ± 0.2	1.0 ± 0.1	4.8 ± 1.1	>100
18j				10.5 ± 2.6	5.2 ± 0.5	3.4 ± 0.4	2.5 ± 0.3	14.4 ± 1.8	>100
(±)- 4 ^d	B	CO	H	0.55 ± 0.15	0.31 ± 0.02	0.10 ± 0.01	0.13 ± 0.04	7.5 ± 1.4	>100
(-)- 4	B	CO	H	0.21 ± 0.02	0.22 ± 0.04	0.07 ± 0.01	0.09 ± 0.01	3.0 ± 0.7	>100
(+)- 4	B	CO	H	17.6 ± 2.1	13.5 ± 1.0	3.4 ± 0.3	4.6 ± 0.2	82.0 ± 18.2	ND
34d ^{d,e}	B	CO	H	10.5 ± 1.2	9.1 ± 1.0	4.9 ± 0.6	6.0 ± 2.0	59.2 ± 19.6	ND
34e ^d	B	CO	Br	0.32 ± 0.01	0.25 ± 0.02	0.10 ± 0.01	0.15 ± 0.01	8.0 ± 2.1	>100
34f ^d	B	CH ₂	H	11.2 ± 1.3	10.3 ± 1.9	2.7 ± 0.1	3.2 ± 0.2	39.0 ± 10.0	ND
34g ^d	C		H	1.5 ± 0.1	0.76 ± 0.11	0.29 ± 0.02	0.57 ± 0.03	14.1 ± 1.6	>100
34h ^d	C		Br	3.9 ± 0.2	2.2 ± 0.3	0.66 ± 0.07	1.0 ± 0.1	11.5 ± 3.0	ND

^aAbbreviations: ND = not determined. ^b K_{B} values (μM) for inhibiting the responses of recombinant rat NMDA (GluN1 expressed with the appropriate GluN2 subunit) receptors expressed in *Xenopus* oocytes (mean ± SEM). For compounds with activities listed as >100 this refers to the IC₅₀ value. ^c K_{B} values for antagonism of glutamate-stimulated Ca²⁺ influx in HEK293 cells expressing either human GluK1 or GluK2 (mean ± SEM). For compounds with activities listed as >100 this refers to the K_{B} value. ^dData for NMDA receptor antagonist activity taken from ref 6. ^eCompound **34d** is the racemic trans isomer of **4**.

derivative (**34h**) had GluK1 affinity similar to that determined for the corresponding unsaturated derivatives (Table 2). Replacement of the carbonyl linker of (±)-**4** with a CH₂ group to give **34f** (Table 2) reduced GluK1 affinity 5-fold probably because of increased rotational freedom. The anthracene substituted derivative **18j** had only 2-fold lower affinity for GluK1 compared to (±)-**4** (Table 2), suggesting that the pocket accommodating these bulky aromatic rings in the LBD of GluK1 is not as tight as that in GluN2D or that the aromatic ring is projecting out of the GluK1 LBD. These conclusions are backed up by the observation that the 3-phenanthryl derivative **5** has affinity similar to that observed for (±)-**4** and **18j** (Table 2). Addition of a halo substituent to the 9-position of the phenanthrene ring of **5** resulted in the following rank order of affinity, I > Br > H > Cl, suggesting that the 9-position substituent is accommodated by a spacious hydrophobic pocket. The 9-bromo derivative **18h** displays ~9-fold selectivity for GluN2D versus GluK1, but the 9-iodo derivative **18i** has almost equal affinity for these two subunits (Table 2).

In the 6-substituted naphthyl series (**18a–d**, **19**, Table 1) the following rank order of affinity was observed on GluK1: Ph > I > Br > H > CO₂H ~ F, suggesting that there is a spacious hydrophobic pocket in the vicinity of the 6-substituent that does not accommodate polar substituents. As was observed in the SAR study on GluN2D the presence of the third aromatic ring in **5** (Table 2) and its derivatives has only a weak enhancing effect on GluK1 affinity when compared to the corresponding 6-substituted naphthyl analogue (e.g., **18i** (Table 2) has only 1.7-fold higher affinity for GluK1 compared to **18c** (Table 1)). The antagonist **18d** (Table 1) that showed reasonable selectivity for GluN2C/GluN2D versus GluN2A/

GluN2B had an affinity for GluK1 similar to that observed for GluN2D.

Replacement of the carbonyl linker of the biphenyl derivative **34b** with a sulfonyl group to give **34c** markedly reduces GluK1 affinity such that this compound shows selectivity for GluN2D versus GluK1 (Table 1). Interestingly, 4'-carboxy substitution of **34b** to give **20** markedly reduces GluN2D affinity but only reduces GluK1 affinity 5-fold, and therefore, **20** is selective for GluK1 versus GluN2D (Table 1). The extent of this selectivity could not be determined because of poor water solubility at higher concentrations. Replacement of the first phenyl ring of (±)-**4** by an ethylene spacer to give **21** reduces GluK1 affinity 9-fold (Table 1). Analogues of *cis*-**34b** where the phenyl rings are joined by an acetylene (**18k**), ethylene (**21**), or diazene (**18l**) spacer had approximately 2-fold lower affinity for GluK1 compared to the parent compound (Table 1). Thus, **18k** and **18l** had similar affinities for GluK1 and GluN2D.

The compounds that displayed the highest affinity for GluK1 were also tested as antagonists of GluK2 receptors. A number of compounds in this series ((±)-**4**, **5**, **18c**, **18d**, **18 h–j**, **18k**, **18l**, (-)-**4**, **34b**, **34e**, and **34g**) show selectivity for GluK1 versus GluK2, as they had no GluK2 antagonist activity when tested at 100 μM (Tables 1 and 2).

Electrophysiological Characterization of the Activity of 18i on Human KAR Subtypes and Native AMPARs. Compound **18i** was one of the most potent of the GluK1 antagonists to be identified in the Ca²⁺ fluorescence assay described above. Because of the rapid and concanavalin A insensitive desensitization of GluK3 receptors upon agonist application, it was not possible to use the Ca²⁺ fluorescence assay to test compounds on GluK3.¹³ Therefore, we tested **18i** across GluK1–3 to assess KAR

subunit selectivity using an electrophysiological assay that relies on fast application of L-glutamate. In these assays **18i** was a moderately potent antagonist of GluK1 with an IC_{50} value of $0.65 \mu\text{M}$ (95% confidence interval of $0.27\text{--}1.7 \mu\text{M}$, $n = 1\text{--}6$), was a much weaker antagonist of GluK3 with an IC_{50} value of $81.3 \mu\text{M}$ (95% confidence interval of $40.5\text{--}163 \mu\text{M}$, $n = 3\text{--}8$), and had only weak activity on GluK2 ($IC_{50} > 100 \mu\text{M}$, $n = 2$). Thus, **18i** has a >100-fold lower IC_{50} for GluK1 versus GluK3 and has only very weak antagonist activity on GluK2 (Figure 2A).

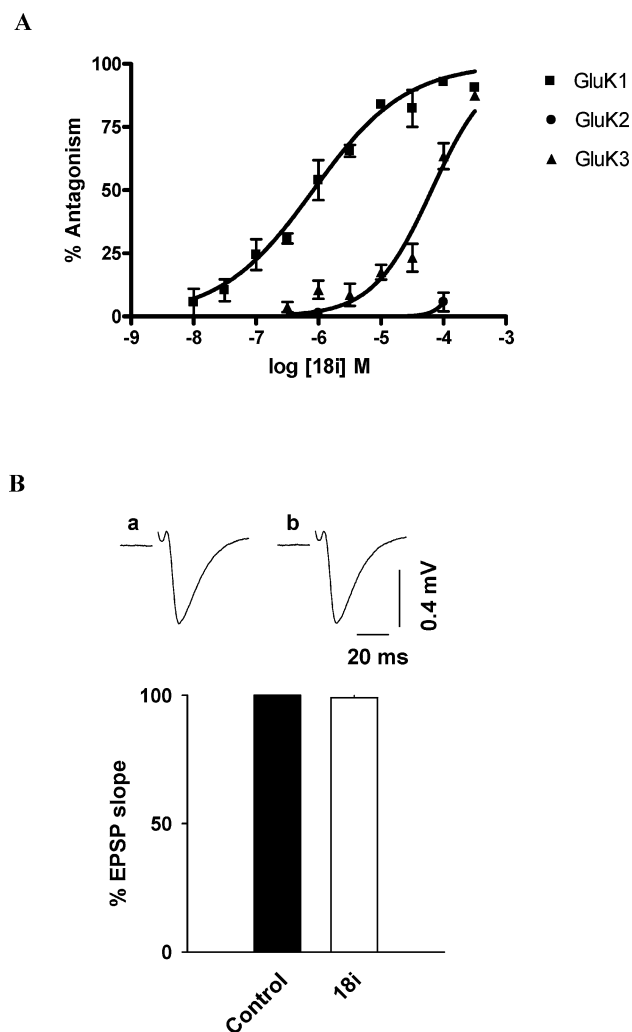


Figure 2. (A) Concentration response curves for the antagonist activity of **18i** in electrophysiological assays on recombinant human GluK1 (■), GluK2 (●), GluK3 (▲), KAR subunits expressed in HEK293 cells. IC_{50} values were estimated to be $0.65 \mu\text{M}$ (95% confidence interval of $0.27\text{--}1.7 \mu\text{M}$, $n = 1\text{--}6$) for GluK1, $>100 \mu\text{M}$ ($n = 2$) for GluK2, and $81.3 \mu\text{M}$ (95% confidence interval of $40.5\text{--}163 \mu\text{M}$, $n = 3\text{--}8$) for GluK3. (B) Pooled data showing the lack of effect of **18i** ($100 \mu\text{M}$) on AMPAR mediated synaptic transmission at mossy fiber synapses following 30 min of perfusion. There was no significant difference ($P = 0.68$, Student's t test) between the control response ($100 \pm 2\%$) and the response in the presence of **18i** ($99 \pm 2\%$). Data are expressed as % of slope (mean \pm SEM, $n = 4$). The inserted traces are averages of four successive responses obtained under (a) control conditions and (b) in the presence of **18i**. Stimulus artifact has been removed for clarification.

Compound **18i** showed no antagonist activity at $100 \mu\text{M}$ ($n = 4$) in an electrophysiological assay on AMPAR mediated excitatory postsynaptic potentials (EPSPs) in the CA3 region of

the hippocampus (Figure 2B). Thus, **18i** shows good selectivity for GluK1 versus GluK2, GluK3, and AMPARs.

Ligand Docking into the LBD of GluK1. To investigate binding modes of some compounds in GluK1, we undertook a molecular modeling study in which the X-ray structure of the LBD of GluK1 in complex with the antagonist **11** (Figure 1) was used as a template.²⁴ Both enantiomers of each of (\pm)-**4** (Table 2), *cis*-**18c** (Table 1) and *cis*-**18i** (Table 2), were docked into the LBD of GluK1 using the Induced Fit workflow within Maestro, which carries out an initial docking using Glide, followed by side chain optimization within 5 \AA of ligand poses with Prime and then a more precise Glide docking in XP mode.²⁵ Only the 2*S*,3*R* isomer of **4** gave satisfactory poses in docking experiments with the LBD of GluK1 (Figure 3A). This is in agreement with the experimental observation that only the (–)-**4** enantiomer had high affinity for GluK1, suggesting that (–)-**4** has the 2*S*,3*R* configuration. This stereoselectivity was also observed in docking studies with the individual isomers of *cis*-**18c** and *cis*-**18i**.

Inspection of the binding modes of the 2*S*,3*R* enantiomers of **4**, **18c**, and **18i** revealed that the piperazine-2,3-dicarboxylic acid nuclei of all ligands adopted the same set of interactions with residues in the LBD of GluK1 (Figure 3) and were similar to those previously reported for interaction with the LBD of GluN2 subunits.²³ The carboxylate group at the 3-position of the piperazine ring forms ionic and hydrogen bond interactions with R508 and a hydrogen bond interaction with T503. The marked reduction in antagonist affinity of **18i** observed for GluK2 compared to GluK1 may be due in part to the switch from T503 in GluK1 to an alanine residue at the equivalent position in GluK2. The carboxylate group at the 2-position of the piperazine ring forms a hydrogen bond with the OH group of S674. This direct interaction may be a major reason for the observed GluK1 versus GluK2 and GluK3 selectivity of **18i** because in the latter two subunits, S674 is replaced by an alanine residue. The positively charged secondary amine forms a hydrogen bond with the carbonyl group of P501. The interaction of the secondary amino group and the carboxylate group adjacent to it in piperazine-2,3-dicarboxylic acid derivatives with residues in the LBD is similar to the way in which the α -amino and α -carboxylate groups of antagonists such as **12** (Figure 1) interact with residues in the X-ray crystal structure of the LBD of GluK1.^{24,26}

Inspection of the binding mode of the 2*S*,3*R* isomer of **4** (Figure 1) to the LBD of GluK1 reveals that the phenanthrene ring is projected straight out of the cleft between the two domains of the LBD toward S706 (Figure 3A). The position of the phenanthrene ring of **4** in the LBD of GluK1 is similar to that previously observed in the LBD of GluN2 subunits. A major reason for the lower affinity of the active enantiomer of **4** for GluK1 versus GluN2A–D is the scarcity of hydrophobic residues in GluK1 with which the phenanthrene ring of **4** can interact. The only hydrophobic residues available are V670, the CH_2 group of N705 and Y474, the latter being above the plane of the phenanthrene ring. This suggests that more of the phenanthrene ring is exposed to water when bound to GluK1 and so less binding energy is gained by loss of ordered water upon ligand binding to the LBD.

The binding mode of the 2*S*,3*R* isomer of **18c** (Table 1) in the LBD of GluK1 (Figure 3B) is similar to that observed in the LBD of GluN2A. However, the binding pocket for the naphthyl ring in GluK1 contains fewer residues, with only the side chains of K473, Y474, and A476 being available to form hydrophobic

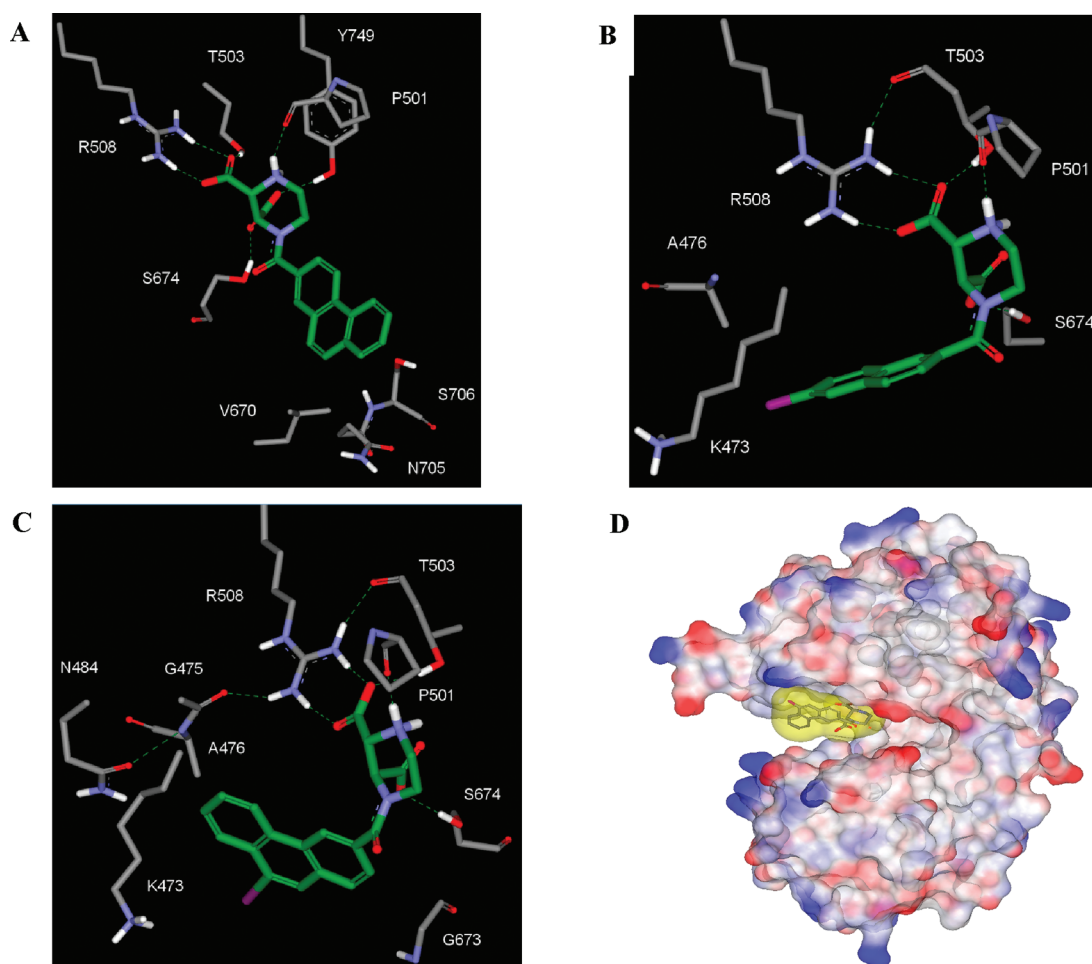


Figure 3. Interactions of ligands with the LBD of GluK1: (A) 2S,3R isomer of **4**; (B) **18c**; (C) **18i**. (D) Solvent accessible surfaces have been calculated for both the LBD of GluK1 and **18i** to show that the ligand is an antagonist of GluK1 because it prevents closure of the ligand binding domain due to the presence of the bulky aromatic substituent.

interactions. The explanation for the observed lower affinity of **18c** for GluK1 compared to GluN2A-D is therefore likely the same as that proposed for **4**. The rank order of affinity for GluK1 observed for 6-halophenyl derivatives was 6-I > 6-Br > 6-F (Table 1). This is consistent with the modeled interaction of **18c** with GluK1 where the larger iodo group is better able to form van der Waals interactions with K473, A476, and N484. The larger 6-phenyl group of **18d** (Table 1) is likely to be able to form more interactions with these residues, and this may explain the slightly higher affinity of **18d** compared to **18c** for GluK1.

The modeled interaction of **18i** (Table 2) with the LBD of GluK1 (Figure 3C) was similar to that observed for **18c** (Table 1). There is less than a 2-fold increase in affinity for GluK1 when comparing **18i** to **18c**, so the extra phenyl ring is not contributing much to the binding energy and this is consistent with the modeled interaction of **18i**, as the distal phenyl ring is mainly pointing out into the solvent water. The 9-iodo group of **18i** occupies a position similar to that of the 6-iodo group of **18c**, and so the observed rank order of affinity of 9-halo substituted derivatives, 9-I > 9-Br > 9-Cl (Table 2), can be explained in the same way as for 6-halo naphthyl derivatives.

Point Mutation Studies to Investigate the Binding of 18i to GluK1 and GluK3. Modeling studies suggested that the GluK1 selectivity of **18i** (Table 2) may be at least in part

due to the binding of the carboxylic acid at the 2-position of the piperazine ring to S674. Reduced binding of **18i** to GluK3 may be due to the switch from S674 in GluK1 to A660 in GluK3, as the alanine residue would not interact favorably with the 3-CO₂⁻ group of **18i**. We investigated this hypothesis by producing the A660S point mutant of rat GluK3. Immunoblot analysis³⁰ confirmed that the A660S mutation did not alter GluK3 protein levels in HEK293 cells compared to wild type (not shown). In contrast to the low binding affinity observed on wild type GluK3, **18i** more potently inhibited [³H]kainate binding to the A660S point mutant of GluK3 (Figure 4), suggesting that it is the switch from S674 in GluK1 to A660 in GluK3 that is primarily responsible for the low affinity of **18i** for GluK3.

Effect of 18i on Nociceptive Behavior in Rats. Both GluN2D and GluK1 have been implicated in neuropathic pain.^{4b,11c,f,12b} We therefore investigated the antinociceptive activity of **18i**, a compound that is a dual GluN2D and GluK1 antagonist. In a mild nerve injury model, acute administration of **18i** completely reversed the drop in mechanical withdrawal threshold seen 1 week after injury (Figure 5A). Thermal hypersensitivity does not develop in animals with partial saphenous nerve ligation injury (PSNI),²⁷ but **18i** increased thermal withdrawal latency in these animals above baseline values

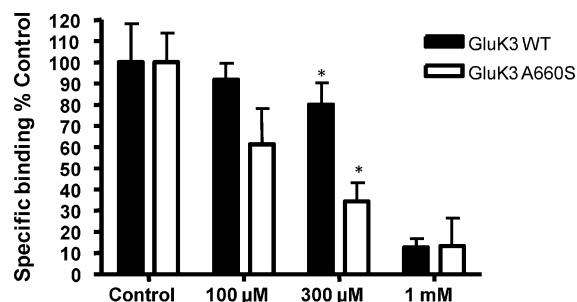


Figure 4. An alanine residue (A660) is a major determinant of the insensitivity of GluK3 to **18i**. In competition binding assays **18i** (100 μ M, 300 μ M, 1 mM) inhibited [3 H]kainate (20 nM) binding to wild type (WT) GluK3 less potently than binding to the GluK3 A660S mutant receptor (data from three separate experiments, each performed in triplicate, mean \pm SEM). Data obtained for 300 μ M **18i** are significantly different for WT GluK3 and GluK3 A660S mutant ($P < 0.05$, Student's t test).

(Figure 5B). **18i** also exerted antinociceptive effects in normal animals before nerve injury (not shown).

DISCUSSION AND CONCLUSIONS

NMDAR antagonists with selectivity for individual GluN2A–D subunits would have utility in determining the functions of these subunits in the CNS and may ultimately have therapeutic applications in a number of neurological disorders.⁴ Although negative allosteric modulators with GluN2C/GluN2D selectivity have been reported,^{8,9} competitive antagonists with good selectivity for GluN2D have been harder to obtain, likely because of the high amino acid sequence homology among the orthosteric LBDs of GluN2A–D.

Structure–Activity Relationship Studies on NMDA Receptors. We have previously reported that N^1 -aryl-substituted derivatives of *cis*-piperazine-2,3-dicarboxylic acid (**17**) (Scheme 1) are competitive NMDAR antagonists and that some of these antagonists have an unusual pattern of subunit selectivity, where they have greater selectivity for GluN2C- or GluN2D-containing NMDARs compared to those containing GluN2A or GluN2B.^{5,6} However, the best compounds identified so far, such as **5** and **18h** (Table 2), only have at most a 10-fold selectivity for GluN2D versus GluN2A and GluN2B. We have therefore synthesized a new range of

N^1 -substituted analogues of **4** and **5** (Table 2) with the aim of gaining more knowledge of the structural requirements for optimal GluN2D selectivity. Of the new compounds that were tested, only **18d** (Table 1) showed greater GluN2D versus GluN2A selectivity compared to **5** and **18h**; however, estimation of the K_i values for antagonist activity at GluN2A and GluN2B was hampered by poor water solubility of this compound at concentrations higher than 100 μ M. Nonetheless, **18d** represents an important lead in developing competitive antagonists with GluN2C/GluN2D selectivity. Other compounds gave insights into the structural requirements for optimal interaction with GluN2D. For instance, we found that only the (–)-**4** enantiomer of (\pm)-**4** had potent antagonist activity at GluN2D subunits (Table 2), and our previously reported modeling studies suggest that this is the 2*S*,3*R* isomer.²³ Unfortunately, we have not been able to obtain confirmation of this configuration through X-ray crystallography, as suitable crystals of (–)-**4** have been impossible to obtain. We have shown that among 9-halo substituted derivatives of **5**, the 9-bromo derivative (**18h**) has greatest selectivity for GluN2D, though the 9-iodo derivative (**18i**) (Table 2) has highest affinity for this subunit. In the 6-halo substituted naphthyl series (**18a–d**, **19**, Table 1) the 6-iodo derivative (**18c**) had the highest affinity for GluN2D but showed little selectivity between the four GluN2 subunits, suggesting that the third phenyl ring of **18h** (Table 2) is important for increasing selectivity for GluN2D.

The ligand binding pocket in GluN2D includes two residues R437 (also present in GluN2C) and R737 (present only in GluN2D) that are not found in GluN2A or GluN2B. We have previously reported modeling and point mutation studies that suggested that the phenanthrene ring of **4** forms hydrophobic contacts with R737, and this likely explains the weak selectivity of this compound for GluN2D.²³ It is likely that similar contacts are made with R737 by the aromatic rings of **5**, **18d**, and **18h**, and this underlies their selectivity for GluN2D versus GluN2A and GluN2B. The fact that most compounds tested show no preference between GluN2C and GluN2D suggests that R437 may also play a role in forming hydrophobic interactions with the aromatic residues of these ligands.

Structure–Activity Relationship Studies on Kainate Receptors. Two benzoyl-substituted derivatives **13** and **14** (Figure 1) have been shown to be nonselective antagonists of

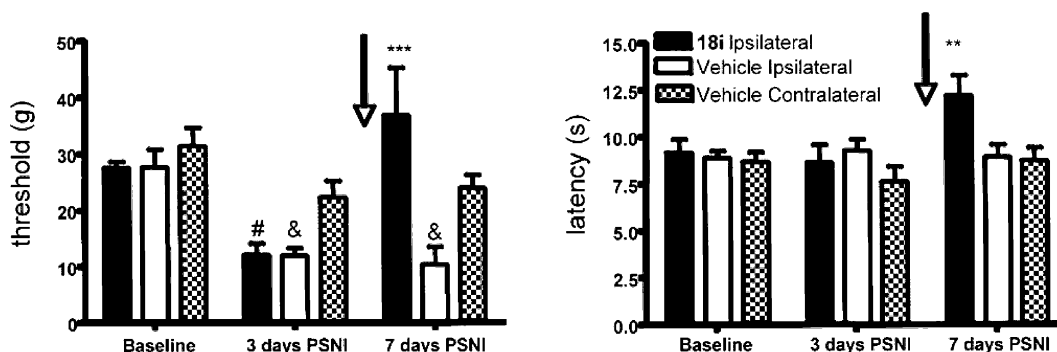


Figure 5. (A, left) **18i** reversed nerve injury induced nociceptive behavior. Male Wistar rats developed significant ipsilateral but no contralateral mechanical allodynia 3 days after PSNI (nerve injury), compared to baseline ((#) $p < 0.01$ and (&) $p < 0.001$ compared to baseline values, one way ANOVA, $n = 5$ per group). Acute administration of 30 mg/kg **18i** ip up to 1 h prior to testing on day 7 (vertical arrow) reversed the allodynia in comparison to vehicle administration ((***) $p < 0.001$, two way ANOVA, $n = 5$ per group). (B, right) Animals with PSNI do not develop thermal hypersensitivity following nerve injury. Acute treatment with **18i** prior to testing on day 7 (arrow) led to an increase in withdrawal latency to radiant heat ((**) $p < 0.01$, two way ANOVA, $n = 5$ per group). All data are shown as the mean \pm SEM.

iGluRs²⁸ and were shown to block kainate-induced responses on isolated dorsal root C-fibers.^{16,28} KARs expressed on these dorsal root C-fibers have been reported to contain the GluK1 subunit.²⁹ We therefore tested the newly synthesized compounds and those whose activity on NMDARs we had reported previously, in a functional assay on recombinant human GluK1 receptors. All of the compounds except **34c** antagonized GluK1 receptors, with **18i**, **18d**, and (–)-**4** being the most potent antagonists tested (Tables 1 and 2). Two of the more selective GluN2D antagonists **5** and **18h** have around 10-fold selectivity for GluN2D versus GluK1 (Table 2); however, the 6-phenyl-naphthyl derivative (**18d**, Table 1), which showed >10-fold selectivity for GluN2D versus GluN2A and GluN2B, had almost equal affinity for GluN2D and GluK1.

The difference in GluK1 activity between the carbonyl (**34b**) and sulfonyl (**34c**) (Table 1) linked biphenyl analogues is likely due to difference in geometry, which would lead to the biphenyl group probing different regions of the GluK1 LBD. Replacement of the carbonyl group with a sulfonyl linker may be a strategy for developing future derivatives with high affinity and selectivity for NMDARs versus GluK1. Two compounds **20** and **21** (Table 1) had little activity on NMDARs when tested at 100 μ M, but **21** in particular had moderate antagonist activity at GluK1. These compounds may be leads for the development of more potent GluK1 selective antagonists.

The compounds with the most potent GluK1 antagonist activity were also tested on recombinant human GluK2 receptors, but none of these compounds were found to have antagonist activity (Tables 1 and 2). One compound, **18i** (Table 2), was tested in electrophysiological assays on HEK293 cells individually expressing GluK1, GluK2, and GluK3. In these assays, **18i** was found to be a relatively potent GluK1 antagonist but had much weaker effects on GluK3 and little or no effect on GluK2 (Figure 2A). Thus, **18i** showed greater selectivity for GluK1 versus GluK3 (>100-fold difference in IC₅₀ values) compared to our previously reported GluK1 antagonists **11** and **12**¹³ (Figure 1).

Modeling and Point Mutation Studies. Modeling studies suggested that the piperazine-2,3-dicarboxylic acid moiety of (–)-**4**, **18c**, and **18i** bound to the LBD of GluK1 in a similar manner to which we have previously proposed for GluN2A-D.²³ The binding mode adopted by (–)-**4**, **18c**, and **18i** in the LBD of GluK1 is unique to this class of compounds. The distal carboxylate of the decahydroisoquinoline and willardiine based antagonists binds deep in the S2 domain of the LBD of GluK1, and it is the spanning of the S1 and S2 domains in the LBD that underlies the foot in the door mechanism of antagonism.²⁶ Compounds (–)-**4**, **18c**, and **18i** have a short interacidic group chain length and cannot reach the deep binding site in the S2 domain that is accessed by the distal acidic group of the decahydroisoquinoline and willardiine based antagonists. Compounds (–)-**4**, **18c**, and **18i** produce their antagonist activity by a different mechanism, as in this case the bulky aromatic substituent blocks the closure of the LBD (Figure 3A–C). A key observation from the modeling study was that S674 in GluK1 was involved in the binding of the carboxylate group at the 2-position of the piperazine ring. We hypothesized that this may underlie the GluK1 versus GluK2 and GluK3 selectivity of **18i**, as the latter two subunits have an alanine residue at the position corresponding to S674 in GluK1 and therefore cannot form a hydrogen bond with the carboxylate group at the 2-position of the piperazine ring of **18i**. Evidence to support this theory came from the observation that

although **18i** had weak activity on wild type GluK3, it had activity on the A660S GluK3 point mutant similar to that observed on GluK1 (Figure 4). It was not possible to test **18i** on the S674A GluK1 point mutant, as both mutant and wild type GluK1 had very low expression levels when transiently transfected into HEK293 cells, as was evident from the very low specific binding of [³H]kainate. Thus, further studies are needed to provide more definitive evidence for the role of S674 in determining the selectivity of **18i** for GluK1 versus GluK2 and GluK3, such as point mutation studies on GluK2 and the acquisition of high resolution crystal structures. The presence of an alanine at position 487 in GluK2 may also contribute to the very low affinity of **18i** for GluK2. In GluK1 and GluK3, this residue is replaced by a threonine residue which makes a hydrogen bond contact with the carboxylate group at the 3-position of the piperazine ring of **18i**. Replacement of this threonine by an alanine would prevent this interaction. Similar reasoning was used to explain the low affinity of willardiine based antagonists, such as **11**, for GluK2.³⁰

Compound 18i Is Selective for KARs versus AMPARs. Compound **18i** was found to be selective for GluK1 versus AMPARs, as it had no effect on AMPARs expressed in the hippocampus (Figure 2B). The lack of effect of **18i** on AMPARs appears to be more general, as we have previously reported that **5**, **18h**, **18k**, and **18l** (Tables 1 and 2) were only very weak inhibitors of [³H]AMPA binding in competition binding assays.^{5c} In the same study we found that 100 μ M **5**, **18h**, **18k**, and **18l** inhibited [³H]kainate binding only 10–20%, but this assay detects activity on multiple KAR subunits and there is a relatively low abundance of GluK1 compared to other KAR subunits in whole brain or forebrain homogenates.³⁰ Thus, **18i** is a selective GluK1 antagonist that may be useful to study the function of KARs containing this subunit, as long as its NMDAR antagonist activity does not interfere. One application could be in the study of NMDAR independent LTP in the CA3 region of the hippocampus, which is known to be dependent on KARs.^{2b}

Antinociceptive Effect of 18i in an Animal Model of Nerve Injury. GluK1 antagonists have been shown to modulate nociceptive function in acute nociceptive and inflammatory models.^{11e} The location of GluK1 on the non-peptidergic population of nociceptive afferents led to the hypothesis that GluK1 antagonists might be effective modulators of neuropathic, as opposed to inflammatory pain.³¹ Likewise, GluN2D-containing receptors have a specific role in neuropathic pain; GluN2D knockout mice do not display enhanced pain responses in the sciatic nerve ligation model.^{4b} Hence, a dual GluK1/GluN2D selective agent would be predicted to have enhanced antinociceptive properties. We have shown that **18i**, administered by intraperitoneal (ip) injection, in an animal model of mild nerve injury completely reversed the drop in mechanical withdrawal threshold seen 1 week after injury and increased thermal withdrawal latency above baseline values (Figure 5). Thus, antagonists such as **18i** with dual activity at GluK1 and NMDARs may have utility in the treatment of neuropathic pain.

Compounds with similar potency as antagonists of GluK1 and NMDARs may have advantages over compounds with either activity alone. For instance, NMDARs and GluK1 containing KARs are known to be involved in pain transmission, epilepsy, and neuronal cell death and dual antagonists may have advantages in the treatment of these disorders, such as improved therapeutic ratios. Intriguingly, with these compounds, it may be

possible to simultaneously optimize both the NMDAR and KAR subtype selectivity appropriate for treating a condition such as neuropathic pain.

In summary, we have identified compounds that could be developed into GluN2D or GluK1 selective antagonists and these may be useful as pharmacological tools to probe the physiological roles of these subunits in the central nervous system. In addition, potent dual antagonists of GluK1 and GluN2D, developed from the leads identified in this study, may have therapeutic application for the treatment of a number of neurological disorders.

EXPERIMENTAL METHODS

Chemistry. General Procedures. Melting points were determined using an Electrothermal IA9100 capillary apparatus and are uncorrected. ^1H NMR spectra were measured on either a Jeol spectrometer at 270.18 MHz, a Jeol JNM-LA300 spectrometer at 300.53 MHz, a Jeol JNM-ECP400 spectrometer at 400.18 MHz, or a Varian 400MR spectrometer at 399.77 MHz. ^{13}C NMR spectra were recorded on either a Jeol JNM-LA300 spectrometer at 75.57 MHz, a Jeol JNM-ECP400 spectrometer at 100.63 MHz, or a Varian 400MR spectrometer at 100.52 MHz. Chemical shifts (δ) are reported in parts per million (ppm) with 3-(trimethylsilyl)propionic-2,2,3,3- d_4 acid sodium salt in D_2O , or tetramethylsilane in CDCl_3 or $\text{DMSO-}d_6$ used as internal standards. Mass spectrometry was performed in the mass spectroscopy laboratories of either the Department of Chemistry, University of Bristol, U.K., or the School of Chemistry, University of Southampton, U.K. Elemental analyses were performed either in the microanalytical laboratories of the Department of Chemistry, University of Bristol, U.K., or by Medac Ltd., Chobham, U.K. The purity of all novel compounds was determined by combustion analysis, which confirmed that they were $\geq 95\%$ pure. Thin layer chromatography was performed on Merck silica gel 60 F_{254} plastic sheets. Flash chromatography was performed on Merck silica gel 60 (220–440 mesh) from Fisher. For thin layer chromatography of amino acids [2 (pyridine/acetic acid/water (3:8:11)):3 (*n*-butanol)] was utilized as the eluent. Amino acids were detected by spraying plates with a 2% solution of ninhydrin in 70% ethanol. The petroleum ether utilized in each case had a boiling point range of 40–60 °C. All anhydrous reactions were conducted under argon. All anhydrous solvents were obtained from Sigma-Aldrich, U.K. (\pm)-4, 5, 17, and 34a–h were synthesized as described previously.⁶

General Procedure for Preparing Acid Chlorides (16c, 16d, 16h, 16i). The appropriate carboxylic acid (7, 15c, 15d, 15h) (1.00 g) was heated under reflux with excess thionyl chloride (5 mL, 68.56 mmol) in anhydrous benzene (40 mL) or anhydrous dioxane (40 mL) under a dry argon atmosphere for up to 12 h. Once all the carboxylic acid had dissolved, the solution was allowed to cool and was subsequently evaporated to dryness under reduced pressure. The product was redissolved in a second aliquot of anhydrous solvent (40 mL), and this was again evaporated to dryness under reduced pressure, ensuring complete removal of any excess thionyl chloride. The acid chlorides (16c, 16d, 16h, 16i) were used without any further purification.

General Procedure for Coupling of Acid Chlorides and *cis*-Piperazine-2,3-dicarboxylic Acid (18c, 18d, 18h, 18i). A solution of the acid chloride in anhydrous dioxane (40 mL) was added dropwise to a rapidly stirring solution of *cis*-piperazine-2,3-dicarboxylic acid (17) and NaOH (3 equiv) dissolved in water/dioxane (1:1) (40 mL) at 0 °C. The reaction mixture was stirred at 0 °C for 2 h and then allowed to warm to room temperature and stirred for a further 4 h. The pH of the reaction mixture was adjusted to 7, diluted to twice the volume with water, and reduced to half volume under reduced pressure. The reaction mixture was acidified to pH 3 with 2 M aqueous HCl, and the precipitate formed was filtered and washed with water and then three times with hot dioxane (50 mL). The solid was redissolved in a minimum volume of 2 M aqueous NaOH, filtered, and precipitated with 2 M aqueous HCl at

pH 3. The resulting solid was collected by filtration, washed with water, and air-dried.

(2*R,3*S**)-1-(6-Iodonaphthalene-2-carbonyl)piperazine-2,3-dicarboxylic Acid (18c).** 15c (1.00 g, 3.36 mmol) and thionyl chloride were reacted in anhydrous benzene. The resulting acid chloride 16c (1.06 g, 3.36 mmol) in anhydrous dioxane and *cis*-piperazine-2,3-dicarboxylic acid (17) (646 mg, 3.36 mmol) and sodium hydroxide (403 mg, 10.08 mmol) in water/dioxane (1:1) afforded 18c as a white solid (272 mg, 18%). Mp: 205–209 °C (dec). ^1H NMR (400 MHz, $\text{D}_2\text{O}/\text{NaOD}$, pH 11) δ 2.43–2.64 (m, 1H), 2.67–2.85 (m, 1H), 2.92–3.05 (m, 1H), 3.14 (d, $J = 3.6$ Hz, 0.5H), 3.20 (d, $J = 3.6$ Hz, 0.5H), 3.32 (d, $J = 13.6$ Hz, 0.5H), 4.17 (dt, $J = 13.6$, 1.6 Hz, 0.5H), 4.56 (d, $J = 3.6$ Hz, 0.5H), 5.35 (d, $J = 3.6$ Hz, 0.5 Hz), 7.33–7.43 (m, 1H), 7.44–7.54 (m, 1H), 7.55–7.71 (m, 2H), 7.76 (s, 0.5H), 7.83 (s, 0.5H), 8.06–8.13 (m, 0.5H), 8.15 (s, 0.5H). MS (ES^-) m/z : 453 (M – H, 100). Anal. ($\text{C}_{17}\text{H}_{15}\text{IN}_2\text{O}_5 \cdot 2.06\text{H}_2\text{O}$) C, H, N.

(2*R,3*S**)-1-(6-Phenyl-naphthalene-2-carbonyl)piperazine-2,3-dicarboxylic Acid (18d).** 15d (1.00 g, 4.03 mmol) and thionyl chloride were reacted in anhydrous benzene. The resulting acid chloride 16d (1.07 g, 4.03 mmol) in anhydrous dioxane and *cis*-piperazine-2,3-dicarboxylic acid (17) (774 mg, 4.03 mmol), sodium hydroxide (322 mg, 8.06 mmol), and sodium carbonate (427 mg, 4.03 mmol) in water/dioxane (1:1) afforded 18d as an off-white solid (455 mg, 28%). Mp: 198–202 °C (dec). ^1H NMR (270 MHz, $\text{D}_2\text{O}/\text{NaOD}$, pH 11) δ 2.81–2.84 (m, 1H), 2.85–3.07 (m, 1H), 3.09–3.27 (m, 1H), 3.31 (d, $J = 3.5$ Hz, 0.5H), 3.38 (d, $J = 3.5$ Hz, 0.5H), 3.52–3.64 (m, 0.5H), 4.29–4.41 (m, 0.5H), 4.79 (usp, 0.5H), 5.54 (d, $J = 3.0$ Hz, 0.5H), 7.41–7.50 (m, 1H), 7.51–7.64 (m, 3H), 7.79–7.87 (m, 2H), 7.88–7.95 (m, 1H), 8.02–8.11 (m, 3H), 8.19–8.24 (m, 1H). MS (ES^-) m/z : 403 (M – H, 100). Anal. ($\text{C}_{23}\text{H}_{20}\text{N}_2\text{O}_5 \cdot 2.88\text{H}_2\text{O}$) C, H, N.

(2*R,3*S**)-1-(9-Bromophenanthrene-3-carbonyl)piperazine-2,3-dicarboxylic Acid (18h).** 15h (1.00 g, 3.32 mmol) and thionyl chloride were reacted in anhydrous benzene. The resulting acid chloride 16h (1.06 g, 3.32 mmol) in anhydrous dioxane and *cis*-piperazine-2,3-dicarboxylic acid (17) (646 mg, 3.32 mmol) and sodium hydroxide (398 mg, 9.96 mmol) in water/dioxane (1:1) afforded the monosodium salt of 18h as an off-white solid (696 mg, 44%). Mp: 232–237 °C (dec). ^1H NMR (400 MHz, $\text{D}_2\text{O}/\text{NaOD}$, pH 11) δ 2.15–2.28 (m, 0.5H), 2.47–2.59 (m, 0.5H), 2.71–2.84 (m, 0.5H), 3.00–3.31 (m, 2H), 3.35 (d, $J = 13.8$ Hz, 0.5H), 3.42 (d, $J = 3.6$ Hz, 0.5H), 4.39 (d, $J = 13.8$ Hz, 0.5H), 4.91 (d, $J = 3.6$ Hz, 0.5H), 5.60 (d, $J = 3.6$ Hz, 0.5H), 6.43–6.68 (m, 2H), 6.86 (s, 1H), 7.04 (s, 1H), 7.12 (s, 1H), 7.45 (s, 1H), 7.82 (s, 1H), 7.94 (s, 1H). MS (ES^-) m/z : 457 (M – H, 100). Anal. ($\text{C}_{21}\text{H}_{16}\text{BrN}_2\text{O}_5 \cdot \text{Na} \cdot 1.61\text{H}_2\text{O}$) C, H, N.

(2*R,3*S**)-1-(9-Iodophenanthrene-3-carbonyl)piperazine-2,3-dicarboxylic Acid (18i).** 7 (1.00 g, 2.87 mmol) and thionyl chloride were reacted in anhydrous benzene. The resulting acid chloride 16i (1.05 g, 2.87 mmol) in anhydrous dioxane and *cis*-piperazine-2,3-dicarboxylic acid (17) (551 mg, 2.87 mmol) and sodium hydroxide (344 mg, 8.61 mmol) in water/dioxane (1:1) afforded 18i as a light orange solid (457 mg, 32%). Mp: 205–210 °C (dec). ^1H NMR (400 MHz, $\text{DMSO-}d_6$) δ 2.86–3.06 (m, 1.5H), 3.64 (usp, 3H), 4.44–4.54 (m, 0.5H), 4.67–4.75 (m, 0.5H), 5.51–5.67 (m, 0.5H), 7.74–7.88 (m, 2.5H), 8.06 (dd, $J = 8.4$, 2.8 Hz, 1H), 8.13–8.21 (m, 1H), 8.67 (s, 0.5H), 8.71 (s, 0.5H), 8.79–8.97 (m, 1.5H), 9.19 (s, 0.5H), 9.35 (s, 0.5H). MS (ES^-) m/z : 503 (M – H, 100). Anal. ($\text{C}_{21}\text{H}_{17}\text{IN}_2\text{O}_5 \cdot 2.06\text{H}_2\text{O}$) C, H, N.

(–)-1-(Phenanthrene-2-carbonyl)piperazine-2,3-dicarboxylic Acid (S)-(–)-1-Phenylethylamine Salt (30). (S)-(–)-1-Phenylethylamine (32) (3.40 mL, 26.44 mmol) was added to a stirred suspension of (\pm)-4 (5.00 g, 13.22 mmol) in water/dioxane (1:1, 100 mL) and the resultant solution allowed to stir for 30 min at room temperature. Concentration in vacuo afforded a white solid, which was suspended in acetone (30 mL), stirred for 10 min, and then filtered to afford a white powder. This was crystallized from boiling water (200 mL) with dioxane being added slowly to the boiling solution until the solid had dissolved (approximately 25 mL). The solution was

filtered while hot and then allowed to stand at room temperature overnight. **30** formed as white crystals which were filtered off and then crystallized a further 3 times until a constant optical rotation was obtained (4.03 g, 61%). $[\alpha]_D^{23} -136^\circ$ (c 0.25, 1:1 dioxane/H₂O). MS (ES⁻) m/z : 377 (M - H, 100). Anal. (C₂₉H₂₉N₃O₅·2.31H₂O) C, H, N.

(-)-1-(Phenanthrene-2-carbonyl)piperazine-2,3-dicarboxylic Acid ((-)-4). **30** (1.00 g, 2.00 mmol) was suspended in THF/water (1:1, 100 mL) and acidified to pH 1 using 2 M aqueous HCl. The THF was removed in vacuo leading to the formation of a white precipitate which was filtered off and washed copiously with cold water. The solid was suspended in ethanol (15 mL) and stirred at room temperature for 10 min. Filtration afforded **(-)-4** as a white solid which was washed with cold ethanol and diethyl ether and then air-dried (607 mg, 80%). $[\alpha]_D^{23} -104^\circ$ (c 0.25, DMSO). Mp: 215–221 °C (dec). ¹H NMR (270 MHz, D₂O/NaOD, pH 11) δ 2.59–3.35 (m, 3H), 3.37 (d, J = 3.6 Hz, 0.5H), 3.45 (d, J = 3.6 Hz, 0.5H), 3.59 (d, J = 13.9 Hz, 0.5H), 4.47 (d, J = 13.9 Hz, 0.5H), 4.79 (usp, 0.5H), 5.57 (d, J = 3.6 Hz, 0.5H), 7.55–8.00 (m, 7H), 8.47–8.71 (m, 2H). MS (ES⁻) m/z : 377 (M - H, 100). Anal. (C₂₁H₁₇N₂O₅Na·1.51H₂O) C, H, N.

(+)-1-(Phenanthrene-2-carbonyl)piperazine-2,3-dicarboxylic Acid (R)-(+)-1-Phenylethylamine Salt (31). **(R)-(+)-1-Phenylethylamine (33)** (3.40 mL, 26.44 mmol) was added to a stirred suspension of **(±)-4** (5.00 g, 13.22 mmol) in water/dioxane (1:1, 100 mL). The resultant solution was allowed to stir at room temperature overnight during which time a white solid precipitated from solution. This was filtered off and washed with water and then acetone. The solid was crystallized from boiling water (200 mL) with dioxane being added slowly to the boiling solution until the solid had dissolved (approximately 10 mL). The solution was filtered hot and then allowed to stand at room temperature overnight. **31** formed as a white solid which was filtered off and then crystallized a further 2 times until a constant optical rotation was obtained (4.42 g, 67%). $[\alpha]_D^{23} +152^\circ$ (c 0.25, 1:1 dioxane/H₂O). MS (ES⁻) m/z : 377 (M - H, 100). Anal. (C₂₉H₂₉N₃O₅·2.18H₂O) C, H, N.

(+)-1-(Phenanthrene-2-carbonyl)piperazine-2,3-dicarboxylic Acid ((+)-4). **31** (1.00 g, 2.00 mmol) was suspended in THF/water (1:1, 50 mL) and acidified to pH 1 using 2 M aqueous HCl. The resultant solution was stirred for 5 min before the pH was adjusted to 3 using 1 M aqueous LiOH. The THF was then removed in vacuo leading to the formation of a white precipitate which was filtered off and washed copiously with cold water followed by ethanol and diethyl ether. Air drying afforded **(+)-4** as a white solid (685 mg, 91%). $[\alpha]_D^{23} +108^\circ$ (c 0.25, DMSO). Mp: 207–213 °C (dec). ¹H NMR (270 MHz, D₂O/NaOD, pH 11) δ 2.48–2.64 (m, 1H), 2.71–2.87 (m, 1H), 2.93–3.23 (m, 1.5H), 3.30–3.45 (m, 1.5H), 4.37 (d, J = 13.0 Hz, 0.5H), 4.79 (usp, 0.5H), 5.54 (d, J = 3.5 Hz, 0.5H), 7.49–7.63 (m, 4H), 7.65–7.71 (m, 1H), 7.73–7.84 (m, 1H), 7.86 (d, J = 1.6 Hz, 0.5H), 8.00 (d, J = 1.6 Hz, 0.5H), 8.38–8.44 (m, 0.5H), 8.46 (d, J = 8.6 Hz, 0.5H), 8.50–8.56 (m, 0.5H), 8.62 (d, J = 8.6 Hz, 0.5H). MS (ES⁻) m/z : 377 (M - H, 100). Anal. (C₂₁H₁₇N₂O₅Na·2.58H₂O) C, H, N.

Modeling Studies. The X-ray crystal structure of **11** (Figure 1) in complex with the LBD of rat GluK1 (PDB code 2F34)²⁴ was used for docking experiments. The structures of the ligands used in docking experiments were built with Maestro, a module of the Schrödinger molecular modeling suite and energy minimized using the MMF94s force field in MacroModel. In all cases carboxylic acids were built in the negatively charged form and the secondary amine was positively charged. Docking of the ligands into the LBD of GluK1 was carried out using the Induced Fit workflow within Maestro, which carries out an initial docking using Glide, followed by side chain optimization within 5 Å of ligand poses with Prime and then a more precise Glide docking in XP mode.²⁵ The centroid of **12** (Figure 1) in the LBD of GluK1 was used to obtain the box center for grid setup to enable Glide docking of ligands into GluK1. All other settings in the Induced Fit workflow were left at default, and the final Glide docking was carried out in XP mode. Ligand poses shown in Figure 3 were prepared using Accelrys DS Visualizer 2.0 (Accelrys, Inc., San Diego, CA, U.S.).

Biology. Electrophysiological Assays Using Recombinant Rat NMDAR Subtypes. Electrophysiological responses were measured using a standard two-microelectrode voltage clamp as previously described.³² The voltage clamp used was a Warner Instruments (Hamden, CT, U.S.) model OC-725B oocyte clamp, designed to provide fast clamp of large cells. The recording buffer contained 116 mM NaCl, 2 mM KCl, 0.3 mM BaCl₂, and 5 mM HEPES, pH 7.4. Response magnitude was determined by the steady plateau response elicited by bath application of 10 μM L-glutamate plus 10 μM glycine at a holding potential of -60 mV. The presence of a plateau response was taken as an indication of the lack of significant activation of the endogenous Cl⁻ current by Ba²⁺ in these cells. Antagonist inhibition curves were fit (GraphPad Prism, ISI Software, San Diego, CA, U.S.) according to the equation $I = I_{\max} - I_{\max}/[1 + (IC_{50}/A)^n]$, where I_{\max} is the current response in the absence of antagonist, A is the antagonist concentration, and IC_{50} is the antagonist concentration producing half-maximal inhibition. Apparent K_i values were determined by correcting for agonist affinity according to the equation $K_i = IC_{50}(\text{obs})/1 + ([\text{agonist}]/EC_{50})$ as described.³³

Calcium Fluorescence Assays Using Recombinant Human KAR Subtypes. The previously characterized HEK293 cell lines stably expressing GluK1(Q)³⁴ or GluK2(Q)³⁵ containing homomeric KARs were used for calcium fluorescence assays. To address the possibility that changes in receptor expression levels over time could influence experimentally determined IC_{50} values, the EC_{50} value for L-glutamate and the IC_{50} values for routinely used control antagonists such as **9** (Figure 1) were continuously monitored, and no significant drift in these values was ever observed. Additionally, cells were never passaged more than 20 times.

Cell growth and ion influx studies using a Flexstation (Molecular Devices, Inc., Sunnyvale, CA, U.S.) were carried out in the presence of concanavalin A exactly as described previously.¹⁵ A range of concentrations of the test compound were prepared in assay buffer containing concanavalin A. During the first run, the plate reader added the test compound, buffer (control wells for subsequent L-glutamate application), or L-glutamate (to obtain a dose-response curve to L-glutamate). During the second run, L-glutamate plus antagonist was added to give a final L-glutamate concentration of either 10 μM (GluK2) or 30 μM (GluK1).

Concentration-response curves were analyzed using GraphPad Prism 3.02 software (San Diego, CA), with slope factor fixed at 1 and with top and bottom fixed at 100% and 0% inhibition, respectively. The dissociation constant (K_B) was calculated according to the Cheng-Prusoff equation³⁶ from the IC_{50} value for inhibiting L-glutamate-induced calcium influx.

Electrophysiological Assays Using Recombinant Human KAR Subtypes. Recombinant homomeric KARs containing GluK1, GluK2, or GluK3 subunits were stably expressed in HEK293 cells.^{34,35,37} Cells were incubated at 37 °C in Dulbecco's modified Eagle medium (DMEM; Sigma, Gillingham, U.K.) supplemented with 2 mM L-glutamine, 10% fetal calf serum, penicillin, and streptomycin. Cells were then plated onto glass coverslips 1–3 days before experiments.

Coverslips plated with HEK293 cells were placed in the experimental chamber and perfused with HEPES buffer solution (HBS) (in mM; 145 NaCl, 2 KCl, 2 MgCl₂, 2 CaCl₂, 10 glucose, 10 HEPES, pH 7.4, 320 mOsm/L) at 20 °C. Patch pipettes were pulled at 1.5–3.5 MΩ and filled with intracellular solution (in mM; 130 CsCH₃SO₃, 2 NaCl, 2 MgCl₂, 10 EGTA, 10 HEPES, 4 Na₂ATP, 0.1 spermine, pH 7.2, 315 mOsm/L). Whole cell patch clamping was performed on single cells, voltage clamped at -70 mV. Cells were then carefully lifted up from the coverslip and placed into the flow of the upper barrel of a θ tube, supplying HBS. The lower barrel supplied 30 mM glutamate. The θ tube was connected to a piezo device, positioned so that its sideways movement would immerse the cell in the glutamate flow for 100 ms. Recordings were taken every 20 s. When the glutamate response had stabilized, six recordings were made and averaged and then an antagonist was applied through both barrels of the θ tube, dissolved to the same concentration in both the HBS and the glutamate. When the drug was in equilibrium, six recordings were made and averaged and then the solutions switched back to the

original solutions to determine the wash off time of the drug. The current setup allows five concentrations of the drug to be tested on each cell, allowing a dose–response curve to be generated for each cell. Antagonists were applied for approximately 2 min or until the response stabilized. Exchange of solutions was complete in 20–40 s.

Electrophysiological Assay on Native AMPARs Expressed in the Hippocampus. Field excitatory postsynaptic potentials (fEPSPs) recordings were performed on transverse rat hippocampal slices (400 μm) using a standard technique.³⁸ Briefly, slices were perfused with extracellular solution containing (mM): NaCl, 124; KCl, 3; NaH_2PO_4 , 1.25; MgSO_4 , 1; NaHCO_3 , 26; D-glucose, 10–15; CaCl_2 , 2; at 29 °C. Recordings were made using microelectrodes containing 3 M NaCl. Synaptic responses were evoked by stimulation of the dentate granule cell layer (mossy fiber pathway) at a baseline interval of 60 s. Data were collected and analyzed online using the WinLTP software (www.ltp-program.com)³⁹. The fEPSPs were signal averaged every 2 min and the slope between 20% and 80% of maximum was measured and plotted online.

Binding Assays on Wildtype and Point Mutated GluK3. Mutagenesis was carried out on human GluK3a encoding cDNAs using the QuikChange XL site-directed mutagenesis kit from Stratagene (La Jolla, CA, U.S.) according to the manufacturer's protocol. All residue numbering excludes the signal peptide. All mutants were verified by full-length sequencing (Geneservice, Oxford, U.K.).

HEK293 cells were maintained in Dulbecco's modified Eagle's medium (Sigma, Gillingham, U.K.) supplemented with 10% (v/v) fetal calf serum (Invitrogen Ltd., Paisley, U.K.), 2 mM L-glutamine, 50 U/mL penicillin, and 50 $\mu\text{g}/\text{mL}$ streptomycin (all from Invitrogen Ltd., Paisley, U.K.) at 37 °C in a humidified atmosphere of 5% CO_2 . Cells were transiently transfected using linear polyethylenimine (PEI; molecular weight $\sim 25\,000$; Polysciences, Warrington, PA).⁴⁰ In brief, DNA and PEI were mixed in 150 mM NaCl at an N/P ratio of 5:8, incubated for 20 min, and added dropwise to cells.

For membrane binding assays, 10 μg of DNA was mixed with 40 μL of PEI (1 mg/mL) in 500 μL of NaCl (150 mM), added to cells in a 175 cm^2 flask, and incubated for 48 h. HEK 293 cells stably transfected with GluK3 were grown in the presence of 0.2 mg/mL hygromycin B (Invitrogen) as described previously.^{34,35,37}

Membrane fractions were prepared from both stably and transiently transfected cells harvested in hypotonic solution (10 mM NaHCO_3 and complete protease inhibitor cocktail; Roche Diagnostics GmbH, Mannheim, Germany) and disrupted using sonication (2×10 s bursts at 10 W, with 20 s incubation on ice in between). Cell homogenates were then spun at 1000g for 20 min at 4 °C to remove cellular debris. Membranes were pelleted at 40000g for 20 min at 4 °C and washed three times by resuspension in binding buffer (50 mM Tris, buffered with citric acid, pH 7.4) and centrifugation (40000g, 20 min, 4 °C). After the measurement of protein concentrations using the Bio-Rad protein assay kit (Bio-Rad Laboratories, Hemel Hempstead, U.K.), membrane fractions were separated into aliquots, snap-frozen in liquid nitrogen, and stored at -80 °C. Ligand binding to wild type and point mutated GluK3 was determined in a filtration binding assay using a Brandel cell harvester (model M-30; Brandel, Gaithersburg, MD) as described previously.⁴¹ Competition binding assays were run with 20 nM [^3H]kainate and 1 mM kainate to determine nonspecific binding. Kainate was obtained from Ascent Scientific (Avonmouth, U.K.). [^3H]Kainate was purchased from PerkinElmer Life and Analytical Sciences. Data were analyzed using GraphPad Prism, version 3.02 (San Diego, CA).

Effect of 18i on Nociceptive Behavior in Rats. Nociceptive behavioral testing was performed on 10 male Wistar rats (~ 250 g). These were kept on a standard 12:12 h light/dark cycle and fed standard chow and water ad libitum. All experimental procedures were carried out in accordance with the United Kingdom Animals (Scientific Procedures) Act 1986 and with the approval of the University of Bristol Ethical Review Panel.

Nerve Injury Surgery. All Wistar rats underwent surgery for nerve injury (PSNI).²⁷ Anesthesia was induced using $\sim 3\%$ isoflurane in oxygen and maintained with $\sim 2\%$ isoflurane in oxygen. Animals were maintained areflexive throughout surgery.

A ~ 1 cm incision was made along the inguinal fossa region (from mid thigh to below knee). Blunt dissection was used to remove superficial connective tissue, and the saphenous nerve was isolated from muscle and vasculature with fine forceps. The saphenous nerve was split and $\sim 50\%$ tightly ligated using sterile 4.0 silk suture. The incision was sutured with sterile 4.0 silk suture, and animals were allowed to recover.

Nociceptive Behavior. Rats were habituated to the testing environment the day prior to testing. All animals underwent a habituation period (10 min) prior to each testing session. Nociceptive testing was carried out after injection of 18i in normal animals prior to saphenous nerve injury and in the same animals once behavioral hypersensitivity had developed, 7 days after PSNI.

Mechanical withdrawal thresholds were measured using calibrated Von Frey (vF) hairs as previously described.²⁷ vF hairs were applied to the plantar surface of the hindpaw for a maximum of 5 s or until the animal withdrew from the stimulus. Each vF hair was applied a total of five times to each hindpaw, and both left and right hindpaws were tested. Stimulus/response curves were constructed and threshold values calculated from these curves.

Standard thermal withdrawal latencies were determined after mechanical nociceptive testing.⁴² The radiant heat source was positioned under the plantar surface of the hindpaw, and latency to withdrawal was recorded. Both right and left hindpaws were tested, and each hindpaw was stimulated a total of three times on each test occasion. A mean of the three measurements was used as the withdrawal latency.

Drug or vehicle ($n = 5/\text{group}$) was administered via intraperitoneal injection, and animals were left for 15 min before nociceptive testing began.

■ ASSOCIATED CONTENT

§ Supporting Information

Experimental procedures and elemental analysis results for intermediates and additional final compounds. This material is available free of charge via the Internet at <http://pubs.acs.org>.

■ AUTHOR INFORMATION

Corresponding Author

*Phone: +44 (0)117 3311409. Fax: +44 (0)1173312288. E-mail: david.jane@bristol.ac.uk

Author Contributions

^{||}M.W.I. and B.M.C. contributed equally as first authors, and D.T.M. and D.E.J. contributed equally as senior authors.

■ ACKNOWLEDGMENTS

The authors thank the NIH (Grant MH60252), the BBSRC (Grant BB/F012519/1), and the MRC (Grants G0601509 and G0601812) for funding this work. The authors thank Dr. David Bleakman at Eli Lilly & Co., U.S., for supplying the GluK1-3 recombinant cell lines.

■ ABBREVIATIONS USED

AMPA, (S)-2-amino-3-hydroxy-5-methyl-4-isoxazolepropanoic acid; AMPAR, (S)-2-amino-3-hydroxy-5-methyl-4-isoxazolepropanoic acid receptor; kainate, (2S,3S,4S)-3-carboxymethyl-4-isopropenylpyrrolidine-2-carboxylic acid; DMEM, Dulbecco's modified Eagle medium; EPSP, excitatory postsynaptic potential; fEPSP, field excitatory postsynaptic potential; HBS, 4-(2-hydroxyethyl)-1-piperazineethanesulfonic acid buffer solution; HEK293, human embryonic kidney 293; HEPES, 4-(2-hydroxyethyl)-1-piperazineethanesulfonic acid; iGluRs, ionotropic glutamate receptors; ip, intraperitoneal; KAR, (2S,3S,4S)-3-carboxymethyl-4-isopropenylpyrrolidine-2-carboxylic acid receptor; LBD, ligand binding domain; LTP, long-term

potentiation; NMDA, *N*-methyl-*D*-aspartic acid; NMDAR, *N*-methyl-*D*-aspartic acid receptor; PEI, polyethylenimine; PSNI, partial saphenous nerve ligation injury; vF, Von Frey; WT, wild type

REFERENCES

- (1) (a) Watkins, J. C.; Jane, D. E. The glutamate story. *Br. J. Pharmacol.* **2006**, *147*, S100–S108. (b) Kew, J. N. C.; Kemp, J. A. Ionotropic and metabotropic glutamate receptor structure and pharmacology. *Psychopharmacology* **2005**, *179*, 4–29. (c) Traynelis, S. F.; Wollmuth, L. P.; McBain, C. J.; Menniti, F. S.; Vance, K. M.; Ogden, K. K.; Hansen, K. B.; Yuan, H.; Myers, S. J.; Dingledine, R. Glutamate receptor ion channels: structure, regulation, and function. *Pharmacol. Rev.* **2010**, *62*, 405–496.
- (2) (a) Collingridge, G. L.; Olsen, R. W.; Peters, J.; Spedding, M. A nomenclature for ligand-gated ion channels. *Neuropharmacology* **2009**, *56*, 2–5. (b) Jane, D. E.; Lodge, D. L.; Collingridge, G. L. Kainate receptors: pharmacology, function and therapeutic indications. *Neuropharmacology* **2009**, *56*, 90–113.
- (3) (a) Monaghan, D. T.; Jane, D. E. Pharmacology of the NMDA Receptor. In *Biology of the NMDA Receptor*; VanDongen, A., Ed.; Taylor and Francis: London, U.K., 2008; pp 257–282. (b) Neyton, J.; Paoletti, P. Relating NMDA receptor function to receptor subunit composition: limitations of the pharmacological approach. *J. Neurosci.* **2006**, *26*, 1331–1333.
- (4) (a) Kalia, L. V.; Kalia, S. K.; Salter, M. W. NMDA receptors in clinical neurology: excitatory times ahead. *Lancet Neurol.* **2008**, *7*, 742–755. (b) Hizue, M.; Pang, C. H.; Yokoyama, M. Involvement of *N*-methyl-*D*-aspartate-type glutamate receptor epsilon I and epsilon 4 subunits in tonic inflammatory pain and neuropathic pain. *NeuroReport* **2005**, *16*, 1667–1670. (c) Sanacora, G.; Zarate, C. A.; Krystal, J. H.; Manji, H. K. Targeting the glutamatergic system to develop novel, improved therapeutics for mood disorders. *Nat. Rev. Drug Discovery* **2008**, *7*, 426–437.
- (5) (a) Buller, A. L.; Monaghan, D. T. Pharmacological heterogeneity of NMDA receptors: characterization of NR1a/NR2D heteromers expressed in *Xenopus* oocytes. *Eur. J. Pharmacol.* **1997**, *320*, 87–94. (b) Feng, B.; Tse, H. W.; Skifter, D. A.; Morley, R. M.; Jane, D. E.; Monaghan, D. T. Structure–activity analysis of a novel NR2C/NR2D-preferring NMDA receptor antagonist: 1-(phenanthrene-2-carbonyl)piperazine-2,3-dicarboxylic acid. *Br. J. Pharmacol.* **2004**, *141*, 508–516. (c) Costa, B. M.; Feng, B.; Tsintsadze, T. S.; Morley, R. M.; Irvine, M. W.; Tsintsadze, V. P.; Lozovaya, N. A.; Jane, D. E.; Monaghan, D. T. NMDA receptor NR2 subunit selectivity of a series of novel piperazine-2,3-dicarboxylate derivatives; preferential blockade of extrasynaptic NMDA receptors in the rat hippocampal CA3-CA1 synapse. *J. Pharmacol. Exp. Ther.* **2009**, *331*, 618–626.
- (6) Morley, R. M.; Tse, H.-W.; Feng, B.; Miller, J. C.; Monaghan, D. T.; Jane, D. E. Synthesis and pharmacology of *N*¹-substituted piperazine-2,3-dicarboxylic acid derivatives acting as NMDA receptor antagonists. *J. Med. Chem.* **2005**, *48*, 2627–2637.
- (7) Fischer, G.; Mutel, V.; Trube, G.; Malherbe, P.; Kew, J. N.; Mohacs, E.; Heitz, M. P.; Kemp, J. A. Ro 25-6981, a highly potent and selective blocker of *N*-methyl-*D*-aspartate receptors containing the NR2B subunit. Characterization in vitro. *J. Pharmacol. Exp. Ther.* **1997**, *283*, 1285–1292.
- (8) Costa, B. M.; Irvine, M. W.; Fang, G.; Eaves, R. J.; Mayo-Martin, M. B.; Skifter, D. A.; Monaghan, D. T.; Jane, D. E. A novel family of negative and positive allosteric modulators of NMDA receptors. *J. Pharmacol. Exp. Ther.* **2010**, *335*, 614–621.
- (9) Mosley, C. A.; Acker, T. M.; Hansen, K. B.; Mullasseril, P.; Andersen, K. T.; Le, P.; Vellano, K. M.; Bräuner-Osborne, H.; Liotta, D. C.; Traynelis, S. F. Quinazolin-4-one derivatives: a novel class of noncompetitive NR2C/D subunit-selective *N*-methyl-*D*-aspartate receptor antagonists. *J. Med. Chem.* **2010**, *53*, 5476–5490.
- (10) Sheardown, M.; Nielsen, E.; Hansen, A.; Jacobsen, P.; Honore, T. 2,3-Dihydroxy-6-nitro-7-sulphamoyl-benzo(F)quinoxaline: a neuroprotectant for cerebral ischemia. *Science* **1990**, *247*, 571–574.
- (11) (a) Clarke, V. R.; Ballyk, B. A.; Hoo, K. H.; Mandelzys, A.; Pellizzari, A.; Bath, C. P.; Thomas, J.; Sharpe, E. F.; Davies, C. H.; Ornstein, P. L.; Schoepp, D. D.; Kamboj, R. K.; Collingridge, G. L.; Lodge, D.; Bleakman, D. A hippocampal GluR5 kainate receptor regulating inhibitory synaptic transmission. *Nature* **1997**, *389*, 599–603. (b) Vignes, M.; Clarke, V. R.; Parry, M. J.; Bleakman, D.; Lodge, D.; Ornstein, P. L.; Collingridge, G. L. The GluR5 subtype of kainate receptor regulates excitatory synaptic transmission in areas CA1 and CA3 of the rat hippocampus. *Neuropharmacology* **1998**, *37*, 1269–1277. (c) Bortolotto, Z. A.; Clarke, V. R.; Delany, C. M.; Parry, M. C.; Smolders, I.; Vignes, M.; Ho, K. H.; Miu, P.; Brinton, B. T.; Fantaske, R.; Ogden, A.; Gates, M.; Ornstein, P. L.; Lodge, D.; Bleakman, D.; Collingridge, G. L. Kainate receptors are involved in synaptic plasticity. *Nature* **1999**, *402*, 297–301. (d) Filla, S. A.; Winter, M. A.; Johnson, K. W.; Bleakman, D.; Bell, M. G.; Bleisch, T. J.; Castano, A. M.; Clemens-Smith, A.; Del Prado, M.; Dieckman, D. K.; Dominguez, E.; Escibano, A.; Ho, K. H.; Hudziak, K. J.; Katofiasc, M. A.; Martinez-Perez, J. A.; Mateo, A.; Mathes, B. M.; Mattiuz, E. L.; Ogden, A. M. L.; Phebus, L. A.; Stack, D. R.; Stratford, R. E.; Ornstein, P. L. Ethyl (3*S*,4*R*,6*S*,8*R*)-6-(4-ethoxycarbonylimidazol-1-ylmethyl)decahydroisoquinoline-3-carboxylic ester: a prodrug of a GluR5 kainate receptor antagonist active in two animal models of acute migraine. *J. Med. Chem.* **2002**, *45*, 4383–4386. (e) Dominguez, E.; Iyengar, S.; Shannon, H. E.; Bleakman, D.; Alt, A.; Arnold, B. M.; Bell, M. G.; Bleisch, T. J.; Buckmaster, J. L.; Castano, A. M.; Prado, M. D.; Escibano, A.; Filla, S. A.; Ho, K. H.; Hudziak, K. J.; Jones, C. K.; Martinez-Perez, J. A.; Mateo, A.; Mathes, B. M.; Mattiuz, E. L.; Ogden, A. M. L.; Simmons, R. M. A.; Stack, D. R.; Stratford, R. E.; Winter, M. A.; Wu, Z.; Ornstein, P. L. Two prodrugs of potent and selective GluR5 kainate receptor antagonists active in three animal models of pain. *J. Med. Chem.* **2005**, *48*, 4200–4203. (f) Weiss, B.; Alt, A.; Ogden, A. M.; Gates, M.; Dieckman, D. K.; Clemens-Smith, A.; Ho, K. H.; Jarvie, K.; Rizkalla, G.; Wright, R. A.; Calligaro, D. O.; Schoepp, D.; Mattiuz, E. L.; Stratford, R. E.; Johnson, B.; Salhoff, C.; Katofiasc, M.; Phebus, L. A.; Schenck, K.; Cohen, M.; Filla, S. A.; Ornstein, P. L.; Johnson, K. W.; Bleakman, D. Pharmacological characterization of the competitive GLUR5 receptor antagonist decahydroisoquinoline LY466195 in vitro and in vivo. *J. Pharmacol. Exp. Ther.* **2006**, *318*, 772–781.
- (12) (a) O'Neill, M. J.; Bond, A.; Ornstein, P. L.; Ward, M. A.; Hicks, C. A.; Hoo, K.; Bleakman, D.; Logde, D. Decahydroisoquinolines: novel competitive AMPA/kainate antagonists with neuroprotective effects in global cerebral ischaemia. *Neuropharmacology* **1998**, *37*, 1211–1222. (b) Simmons, R. M. A.; Li, D. L.; Hoo, K. H.; Deverill, M.; Ornstein, P. L.; Iyengar, S. Kainate GluR5 receptor mediates the nociceptive response to formalin in the rat. *Neuropharmacology* **1998**, *37*, 25–36. (c) O'Neill, M. J.; Bogaert, L.; Hicks, C. A.; Bond, A.; Ward, M. A.; Ebinger, G.; Ornstein, P. L.; Michotte, Y.; Lodge, D. LY377770, a novel iGluR5 kainate receptor antagonist with neuroprotective effects in global and focal cerebral ischaemia. *Neuropharmacology* **2000**, *39*, 1575–1588. (d) Smolders, I.; Bortolotto, Z. A.; Clarke, V. R. J.; Warre, R.; Khan, G. M.; O'Neill, M. J.; Ornstein, P. L.; Bleakman, D.; Ogden, A.; Weiss, B.; Stables, J. P.; Ho, K. H.; Ebinger, G.; Collingridge, G. L.; Lodge, D.; Michotte, Y. Antagonists of GLUK5-containing kainate receptors prevent pilocarpine-induced limbic seizures. *Nat. Neurosci.* **2002**, *5*, 796–804.
- (13) Perrais, D.; Pinheiro, P. S.; Jane, D. E.; Mulle, C. Antagonism of recombinant and native GluR7-containing kainate receptors. *Neuropharmacology* **2009**, *56*, 131–140.
- (14) (a) Dolman, N. P.; Troop, H. M.; More, J. C. A.; Alt, A. J.; Ogden, A. M.; Jones, S.; Morley, R. M.; Roberts, P. J.; Bleakman, D.; Collingridge, G. L.; Jane, D. E. Synthesis and pharmacology of willardiine derivatives acting as antagonists of kainate receptors. *J. Med. Chem.* **2005**, *48*, 7867–7881. (b) Dolman, N. P.; More, J. C. A.; Alt, A.; Ogden, A. M.; Troop, H. M.; Bleakman, D.; Collingridge, G. L.; Jane, D. E. Structure–activity relationship studies on *N*³-substituted willardiine derivatives acting as AMPA or kainate receptor antagonists. *J. Med. Chem.* **2006**, *49*, 2579–2592.
- (15) More, J. C. A.; Nistico, R.; Dolman, N. P.; Clarke, V. R. J.; Alt, A. J.; Ogden, A. M.; Buelens, F. P.; Troop, H. M.; Kelland, E. E.; Pilato, F.; Bleakman, D.; Bortolotto, Z. A.; Collingridge, G. L.; Jane, D. E.

Characterisation of UBP296; a novel, potent and selective kainate receptor antagonist. *Neuropharmacology* **2004**, *47*, 46–64.

(16) Evans, R. H.; Evans, S. J.; Pook, D. C.; Sunter, D. C. A comparison of excitatory amino acid antagonists acting at primary afferent C fibres and motoneurons of the isolated spinal cord of the rat. *Br. J. Pharmacol.* **1987**, *91*, 531–537.

(17) Wendt, M. D.; Rockway, T. W.; Geyer, A.; McClellan, W.; Weitzberg, M.; Zhao, X.; Mantei, R.; Nienaber, V. L.; Stewart, K.; Klinghofer, V.; Giranda, V. L. Identification of novel binding interactions in the development of potent, selective 2-naphthamide inhibitors of urokinase. Synthesis, structural analysis, and SAR of N-phenyl amide 6-substitution. *J. Med. Chem.* **2004**, *47*, 303–324.

(18) Summers, J. B.; Mazdiyasi, H.; Holms, J. H.; Ratajczyk, J. D.; Dyer, R. D.; Carter, G. W. Hydroxamic acid inhibitors of 5-lipoxygenase. *J. Med. Chem.* **1987**, *30*, 574–580.

(19) Adcock, W.; Wells, P. R. Substituent effects in naphthalene. *Aust. J. Chem.* **1965**, *18*, 1351–1364.

(20) Schultz, J.; Goldberg, M. A.; Ordas, E. P.; Carsch, G. Attempts to find new antimalarials. XI. Derivatives of phenanthrene, III. Amino alcohols derived from 9-chlorophenanthrene. *J. Org. Chem.* **1946**, *11*, 320–328.

(21) Mosettig, E.; Van de Kamp, J. Studies in the phenanthrene series. II. Phenanthrene carboxylic acids and 9-bromophenanthrene derivatives. *J. Am. Chem. Soc.* **1932**, *54*, 3328–3337.

(22) Klapars, A.; Buchwald, S. L. Copper-catalyzed halogen exchange in aryl halides: an aromatic Finkelstein reaction. *J. Am. Chem. Soc.* **2002**, *124*, 14844–14845.

(23) Kinarsky, L.; Feng, B.; Skifter, D.; Morley, R. M.; Sherman, S.; Jane, D. E.; Monaghan, D. T. Identification of subunit-specific and antagonist-specific amino acids in the NMDA receptor glutamate binding pocket. *J. Pharmacol. Exp. Ther.* **2005**, *313*, 1066–1074.

(24) Mayer, M. L.; Ghosal, A.; Dolman, N. P.; Jane, D. E. Crystal structures of the kainate receptor GluR5 ligand binding core dimer complex with novel selective antagonists. *J. Neurosci.* **2006**, *26*, 2852–2861.

(25) Schrödinger Suite 2010 Induced Fit Docking Protocol: Glide, version 5.6; Schrödinger, LLC: New York, NY, 2010. Prime, version 2.2; Schrödinger, LLC: New York, NY, 2010.

(26) Alushin, G. M.; Jane, D. E.; Mayer, M. L. Binding site and ligand flexibility revealed by high resolution crystal structures of GluK1 competitive antagonists. *Neuropharmacology* **2011**, *60*, 126–134.

(27) Hulse, R.; Wynick, D.; Donaldson, L. F. Characterisation of a novel neuropathic pain model in mice. *NeuroReport* **2008**, *19*, 825–829.

(28) Pook, P.; Brugger, F.; Hawkins, N. S.; Clark, K. C.; Watkins, J. C.; Evans, R. H. A comparison of the actions of agonists and antagonists at non-NMDA receptors of C fibres and motoneurons of the immature rat spinal cord in vitro. *Br. J. Pharmacol.* **1993**, *108*, 179–184.

(29) (a) Bettler, B.; Boulter, J.; Hermans-Borgmeyer, I.; O'Shea-Greenfield, A.; Deneris, E. S.; Moll, C.; Borgmeyer, U.; Hollman, M.; Heinemann, S. Cloning of a novel glutamate receptor subunit, GluR5: expression in the central nervous system during development. *Neuron* **1990**, *5*, 583–595. (b) Wilding, T. J.; Huettner, J. E. Functional diversity and developmental changes in rat neuronal kainate receptors. *J. Physiol.* **2001**, *532.2*, 411–421. (c) Kerchner, G. A.; Wilding, T. J.; Huettner, J. E.; Zhuo, M. Kainate receptor subunits underlying presynaptic regulation of transmitter release in the dorsal horn. *J. Neurosci.* **2002**, *22*, 8010–8017.

(30) Atlason, P. T.; Scholefield, C. L.; Eaves, R. J.; Mayo-Martin, M. B.; Jane, D. E.; Molnár, E. Mapping the ligand binding sites of kainate receptors: molecular determinants of subunit-selective binding of the antagonist [³H]UBP310. *Mol. Pharmacol.* **2010**, *78*, 1036–1045.

(31) Lucifora, S.; Willcockson, H. H.; Lu, C. R.; Darstein, M.; Phend, K. D.; Valtschanoff, J. G.; Rustioni, A. Presynaptic low- and high-affinity kainate receptors in nociceptive spinal afferents. *Pain* **2006**, *120*, 97–105.

(32) Buller, A. L.; Larson, H. C.; Schneider, B. E.; Beaton, J. A.; Morrisett, R. A.; Monaghan, D. T. The molecular basis of NMDA

receptor subtypes: native receptor diversity is predicted by subunit composition. *J. Neurosci.* **1994**, *14*, 5471–5484.

(33) Durand, G. M.; Gregor, P.; Zheng, X.; Bennett, M. V.; Uhl, G. R.; Zukin, R. S. Cloning of an apparent splice variant of the rat N-methyl-D-aspartate receptor NMDAR1 with altered sensitivity to polyamines and activators of protein kinase C. *Proc. Natl. Acad. Sci. U.S.A.* **1992**, *89*, 9359–9363.

(34) Korczak, B.; Nutt, S. L.; Fletcher, E. J.; Hoo, K. H.; Elliott, C. E.; Rampersad, V.; McWhinnie, E. A.; Kamboj, R. K. cDNA cloning and functional properties of human glutamate receptor EAA3 (GluR5) in homomeric and heteromeric configuration. *Recept. Channels* **1995**, *3*, 41–49.

(35) Hoo, K. H.; Nutt, S. L.; Fletcher, E. J.; Elliott, C. E.; Korczak, B.; Deverill, R. M.; Rampersad, V.; Fantaske, R. P.; Kamboj, R. K. Functional expression and pharmacological characterization of the human EAA4 (GluR6) glutamate receptor: a kainate selective channel subunit. *Recept. Channels* **1994**, *2*, 327–337.

(36) Cheng, Y. C.; Prusoff, W. H. Relationship between the inhibition constant (K_i) and the concentration of inhibitor which causes 50 per cent inhibition (IC_{50}) of an enzymatic reaction. *Biochem. Pharmacol.* **1973**, *22*, 3099–3108.

(37) Nutt, S. L.; Hoo, K. H.; Rampersad, V.; Deverill, R. M.; Elliott, C. E.; Fletcher, E. J.; Adams, S. L.; Korczak, B.; Foldes, R. L.; Kamboj, R. K. Molecular characterization of human EAA5 (GluR7) receptor: a high-affinity kainate receptor with novel potential RNA editing sites. *Recept. Channels* **1994**, *2*, 315–326.

(38) Bortolotto, Z. A.; Amici, M.; Anderson, W. W.; Isaac, J. T.; Collingridge, G. L. Synaptic Plasticity in the Hippocampal Slice Preparation. In *Current Protocols in Neuroscience*; Wiley: Somerset, NJ, 2011; Chapter 6, Unit 6.13.

(39) Anderson, W. W.; Collingridge, G. L. Capabilities of the WinLTP data acquisition program extending beyond basic LTP experimental functions. *J. Neurosci. Methods* **2007**, *162*, 346–356.

(40) Durocher, Y.; Perret, S.; Kamen, A. High-level and high-throughput recombinant protein production by transient transfection of suspension-growing human 293-EBNA1 cells. *Nucleic Acids Res.* **2002**, *30*, E9.

(41) Molnár, E.; Baude, A.; Richmond, S. A.; Patel, P. B.; Somogyi, P.; McIlhinney, R. A. J. Biochemical and immunocytochemical characterization of antipeptide antibodies to a cloned GluR1 glutamate receptor subunit: cellular and subcellular distribution in the rat forebrain. *Neuroscience* **1993**, *53*, 307–326.

(42) Hargreaves, K.; Dubner, R.; Brown, F.; Flores, C.; Joris, J. A new and sensitive method for measuring thermal nociception in cutaneous hyperalgesia. *Pain* **1988**, *32*, 77–88.